NASA CONTRACTOR REPORT

NASA CR-2035

PLANETARY RESONANCES, BI-STABLE OSCILLATION MODES, AND SOLAR ACTIVITY CYCLES

by H. P. Sleeper, Jr.

Prepared by
NORTHROP SERVICES, INC.
Huntsville, Ala. 35807
for George C. Marshall Space Flight Center

NATIONAL AERONAUTICS AND SPACE ADMINISTRATION • WASHINGTON, D. C. • APRIL 1972

TECHNICAL REPORT

1. REPORT NO.	2. GOVERNMENT ACCESSION NO.	3. RECIPIENT'S CATALOG NO.
CR-2035		

4. TITLE AND SUBTITLE	5. REPORT DATE
PLANETARY RESONANCES, BI-STABLE OSCILLATION MODES, AND SOLAR ACTIVITY CYCLES	April 1972
	6. PERFORMING ORGANIZATION CODE
7. AUTHOR(S)	8. PERFORMING ORGANIZATION REPORT #
H. P. Sleeper, Jr.	TR-241-1053
9. PERFORMING ORGANIZATION NAME AND ADDRESS	10. WORK UNIT NO.
Northrop Services, Inc. P. O. Box 1484 Huntsville, Alabama 35807	11. CONTRACT OR GRANT NO. NAS8-21810
	13. TYPE OF REPORT & PERIOD COVERED
12. SPONSORING AGENCY NAME AND ADDRESS	Contractor Report
NASA Washington, D. C.	14. SPONSORING AGENCY CODE

15. SUPPLEMENTARY NOTES

Technical Coordinator: Harold C. Euler, Space Environment Branch, Aerospace Environment Division, Aero-Astrodynamics Lab, Marshall Space Flight Center

16. ABSTRACT

The natural resonance structure of the planets in the solar system yields resonance periods of 11.08 and 180 years. The 11.08-year period is due to resonances of the sidereal periods of the three inner planets. The 180-year period is due to synodic resonances of the four major planets. The 11.08-year and the 180-year periods have been observed in the sunspot time series. The 11-year sunspot cycles from 1 - 19 are separated into categories of positive and negative cycles, Mode I and Mode II cycles, and typical and anomalous cycles. Each of these categories has a characteristic shape, magnitude or duration so that statistical prediction techniques are improved when a cycle can be classified in a given category. These categories are consistent with observed 22-, 80-, or 100-year, and 180-year solar cycles. The presence of these different categories provides evidence for bi-stable modes of oscillation of the sun. The sequence of cycle 20, together with current data on shape and magnitude, suggests that it is a Mode II negative cycle of anomalous duration. On this basis, the next minimum is expected in 1977 and the next maximum is expected in 1981 or later. These epoch values are 2.5 years later than those based on typical cycle characteristics. The time series cycle classification assumes that the Hale 22-year magnetic cycle has failed to occur twice in the last 220 years, and will fail to occur for cycle 21. This assumption is supported by the correlation of magnetic cycle phase changes with a planetary dynamic variable, the statistical treatment of odd and even cycles compared with the postulated positive and negative cycles, and the improved statistics for shape and magnitude with the new classification. Independent information on the polar magnetic field characteristics of cycle 20 also suggests that it is an anomalous cycle.

(Continued on reverse side)

17. KEY WORDS	18. DISTRIBUTION STATEMENT
1, Solar Activity 2, Sun Spots 3, Solar Cycle	

19. SECURITY CLASSIF. (of this report)	20. SECURITY CLASSIF. (of this page)	21. NO. OF PAGES	22. PRICE
Unclassified	Unclassified	56	$3.00

For sale by the National Technical Information Service, Springfield, Virginia 22151

The details of the planetary-solar coupling mechanism have not been well established. Mechanisms usually suggested depend on tidal forces, centrifugal forces, or Coriolis forces on the sun. An alternate model is proposed which depends on synodic spin-orbit coupling of the rigid-rotating core of the sun, and twice the sidereal period of the earth. The mean synodic rotation period of the core is 27.0 days. The Babcock magnetic model is modified, with two or more subcycles, with the presence of equatorial and polar convection zone circulation cells. This framework provides a basis for understanding bi-stable oscillation modes of the sun and provides a new interpretation of Spoerer's law.

The bi-stable modes of oscillation are two stable oscillation modes, analogous to summer and winter oscillation states of the earth's atmosphere. These different modes have different characteristics which can be demonstrated statistically.

FOREWORD

This report presents the results of a study which develops a new statistical method for long-range forecasting of solar activity, based upon planetary resonance periods in the sunspot time series. The study was conducted by Northrop Services, Inc., Huntsville, Alabama, for the National Aeronautics and Space Administration, George C. Marshall Space Flight Center, Aero-Astrodynamics Laboratory, under Contract NAS8-21810, Appendix A-1, Schedule Order No. 5. This work was under the direction of the Space Environment Branch, with Mr. Harold Euler as NASA/MSFC Technical Coordinator.

ACKNOWLEDGEMENTS

The computational aid of Mrs. J. A. Scissum and Mr. K. Rowe is gratefully acknowledged. The interest and support of Mr. R. E. Smith and Mr. W. W. Vaughan is especially appreciated.

TABLE OF CONTENTS

LIST OF ILLUSTRATIONS

Section I

INTRODUCTION

This report deals with the problem of long range prediction of solar activity, i.e., forecasts from 10 to 20 years in advance. Since the discovery of the mean 11-year cycle, much effort has been expended in developing a technique for making accurate long-range predictions of the solar cycle with comparatively little success.

Developing better prediction methods would provide information required for improved models of the structure and activity of the sun, and for improved ability to make forecasts in many areas of geophysics. The solar models which require better information are either physical or phenomenological in character. The geophysical areas which require improved forecast techniques include studies in cosmic-ray intensities, thermospheric phenomena, ionospheric phenomena, lower atmospheric phenomena, and climatic phenomena.

The current solar models include physical models based on the characteristics of the sun's internal structure, and phenomenological models based on the sun's structure and/or external synchronizing sources. The galactic cosmic-ray intensity is correlated inversely with helio-magnetic fluctuations associated with the solar activity cycle. The lower atmosphere, i.e., stratosphere and troposphere, is affected through ozone and C-14 content, and climatic changes appear to be related to long-period, mean solar activity. The ionization of the E and F regions of the ionosphere is controlled by solar EUV, x-ray, charged particle radiation, and solar wind transients. The temperature and density of the thermosphere are strongly controlled by the mean solar activity, transient flare, and magnetic storm activity. Finally, some recent information indicates that secular variations of the earth's non-dipole magnetic field, changes in the mean rotation rate, and active seismic periods may be correlated with the 22-year solar activity cycles and longer term periods. Thus a large number of fields are affected by our knowledge of the solar cycle and its predictability.

1.1 SOLAR CYCLE PREDICTION METHODS

Methods for predicting the solar cycle are generally based on:

- Development of physical or phenomenological models
- Analysis of nonstationary sunspot time series data
- Correlation of sunspot cycle parameters with predictable physical variables.

A relatively complete review of solar activity prediction techniques is given by Vitinski (1962), as well as a current summary of the state-of-the-art, Vitinski (1969).

Development of phenomenological models achieved a major advance with Babcock's (1961) model of the interaction of the sun's poloidal magnetic field with the differential rotation of the surface plasma of the sun. This model has been improved considerably by Leighton (1969), but is still basically a phenomenological model, with parameters adjusted to agree with an average solar cycle. Steenbeck and Krause (1969) have recently developed more complex dynamo models of the sun. These models assume a rigid core rotating with a velocity faster than the surface of the sun. The surface region may rotate rigidly or with differential latitudinal rotation. A radial transition region may or may not be present. The principal consequence of these models is that in addition to the 11-year bi-polar magnetic structure, there is a magnetic quadrupolar component with a typical period of ~~80-100~~ 100-200 years. These models account for the quadrupole magnetic field structure observed near sunspot maximum, and suggest the probable importance of secular cycles in the sunspot time series. However, to date they do not specify uniquely the secular variations in solar activity.

Analysis of the nonstationary sunspot time series has received considerable attention over the years; however, prediction techniques developed on this basis have been relatively unsuccessful to date. Various analytical techniques used have been autocorrelation, harmonic analysis, periodogram analysis, etc. A basic problem has been the limited number of solar cycles available for analysis, i.e., 12 cycles since Wolf's definition of the

relative sunspot number and 19 cycles since the measurement of monthly average sunspot numbers. One of the most promising prediction methods due to King-Hele (1966), based on an assumed 80-year secular cycle of the rise-time from 11-year cycle minimum to maximum, has recently failed for cycle 20. The predicted rise-time was 3.4 years, versus a measured rise-time of 4.1 years.

Correlation of solar cycle parameters with predictable physical variables, i.e., causal models with planetary gravitational or dynamic variables, has also been the subject of an extensive search. The lack of a simple correlation with planetary periods limited the interest in these models until Bigg (1967) demonstrated the correlation of the sunspot numbers with the period of Mercury and the determination of associated effects with periods of other planets, notably Jupiter. The association of the 11.08-year mean solar cycle period with a planetary tidal period of 11.08 years by Wood and Wood (1965) also suggested a planetary mechanism. Shuvalov (1970) has studied 11-year and 100-year planetary resonances with respect to the solar cycle and its secular variations. Finally, Suda (1962) and Jose (1965) have studied a 180-year period in the sunspot series which they associate with a corresponding 180-year planetary resonance period. Jose suggests a correlation between solar cycle characteristics and the rate of change of the angular momentum of the sun about the center of mass of the solar system.

1.2 OBJECTIVES

The objectives of this report are:

- To use a planetary resonance hypothesis as a basis for an improved forecasting method
- To use linear regression statistical forecasts as a basis for assessing the degree of improvement
- To obtain unique forecasts in order to test the basic validity of the technique
- To examine the consequences, and develop a new phenomenological solar cycle model
- To predict the characteristics of cycles 20 and 21.

The methods which are currently being used to predict solar cycle behavior are linear regression forecasts based upon the statistical analysis of previous cycles. The original technique was developed by McNish and Lincoln (1949). Different authors use different lengths of the past data series for forecast purposes (Weidner, 1969; Lincoln, 1970; Stewart and Ostrow, 1970). The principal assumptions are that there is no correlation between cycles, and that the data are normally distributed. This publication is an extension of the work presented in previous reports by Sleeper (1970 and 1971).

Section II

PLANETARY RESONANCE CHARACTERISTICS AND CLASSIFICATION OF CYCLES

The results of this study are based on the working hypothesis of an interaction of the planets with the sun. No specific interaction model is assumed, but it is anticipated that planetary gravitational or dynamic effects can produce sensible effects in the sun's chromosphere, which in turn have a significant effect on gravity waves in the photosphere. The general physical process envisioned is analogous to the timing control of bi-stable oscillation modes in the earth's stratosphere (Quasi-biennial Oscillation) by the small amplitude six-month oscillation in the upper atmosphere (Lindzen and Holton, 1968).

This section of the report discusses recent developments in the resonance theory of the structure of the solar system, the effect of the resonance structure on the classification of cycles, and the study of supporting data for the choice of cycle classification.

2.1 PLANETARY RESONANCE CHARACTERISTICS

One of the stated objectives of this paper is to utilize a correlation between the sunspot time series and planetary characteristics. An implicit assumption is that if there are fundamental resonant planetary periods, there will be a corresponding resonance structure in the sunspot time series.

The aim of establishing relatively simple resonance or harmonic relationships between the periods of the planets has been of scientific interest for a very long time. Kepler (1619) devoted a large part of his scientific effort to develop a basis for "the music of the spheres." The recent experimental work on the quantized rotation rates of Venus and Mercury, and the theoretical work of Goldreich, Alfven and Molchanov, has provided the framework for an appreciation of the resonance structure of the solar system. Molchanov's development of a resonance system in terms of six quantum numbers provides a basis for treating the solar system by methods analogous to the Bohr model

of the atom. The existence of the planetary resonances provides a framework for understanding the 11-year and the 180-year solar activity periods.

The first significant approach to this problem was that of Titus of the Wittenberg Observatory, and is known as Bode's law:

$$a_n = b + c\ 2^n$$

$$n = -\infty, 0, 1, 2, \ldots$$

where a_n is the semi-major axis of the planetary orbits. While this law worked well for predicting the orbits of Uranus and the asteroids, it failed for Neptune so no fundamental significance has been attributed to it.

Recent experimental work on the rotation rates of Venus and Mercury and theoretical work on gravitational resonance theory by Goldreich (1965, 1966) and Alfven and Arrhenius (1970) have led to the study of previously unexpected resonances. These include orbit-orbit coupling of the satellites of the larger planets, spin-orbit coupling of the rotation rate of Mercury with its orbital period, and the possible spin-orbit coupling of Venus with the synodic period of Venus and Earth. The existence of this latter resonance is still in doubt (Carpenter, 1970). However, from these studies it is apparent that relatively small gravitational forces can have significant effects previously unsuspected.

One of the most recent empirical and theoretical studies of the resonance structure of the solar system is due to Molchanov (1968). He determined the resonance relations for the planets in terms of the reference frequency of Jupiter and six "quantum" numbers: 1, 2, 3, 5, 6, 7. The frequencies of the planets, w_n, are then given by the following set of eight simultaneous equations:

$$\omega_1 - \omega_2 - 2\omega_3 - \omega_4 = 0$$
$$\omega_2 - 3\omega_4 - \omega_6 = 0$$
$$\omega_3 - 2\omega_4 + \omega_5 - \omega_6 + \omega_7 = 0$$
$$\omega_4 - 6\omega_5 - 2\omega_7 = 0$$
$$2\omega_5 - 5\omega_6 = 0$$
$$\omega_5 - 7\omega_7 = 0$$
$$\omega_7 - 2\omega_8 = 0$$
$$\omega_7 - 3\omega_9 = 0$$

The frequencies determined by these resonance relations agree with the planetary frequencies within 1.2 percent. A similar analysis for the orbits of the satellites of Jupiter, Saturn and Uranus demonstrate their resonance structure. The resonance structure observed is obtained in principle from a theoretical treatment of the solar system in an early nebula stage of development. Under those conditions, nebular viscosity provides a mechanism for nonlinear interaction between pairs of condensations, with resonant conditions being a necessary consequence. Molchanov's further analysis (1969 a, b) indicates that the probability of the occurrence of these resonance relations by chance is less than 10^{-4} for the planets and less than 10^{-11} when the satellite resonances are included.

An additional consequence of the resonance structure of the solar system is the presence of two unique harmonics of the system, 11.08 years and 178 years. The resonances corresponding to these periods are given in Tables 2-1 and 2-2 (Blizard, 1969). Additional resonances with a period of 100 years are given by Shuvalov (1970). Apropos of Blizard's planetary resonances, it appears that the lunar synodic period is more nearly commensurate with the 11.08-year period than is the earth's orbital period, or the earth should be treated as a double planet.

2.2 PLANETARY RESONANCE AND STRUCTURE IN THE SUNSPOT TIME SERIES

The search for structure in the sunspot time series has been very extensive and no attempt will be made to give a complete review here. However, the basic structure which has been detected will be discussed as a foundation for cycle classification and further analysis.

The annual running mean of the Zurich relative sunspot number, R_Z, from 1700 to 1970 is given in Figure 2-1. The Wolf number was defined in 1849 and equivalent numbers have been derived from monthly average numbers back to 1749 (Waldmeier, 1961). Previous numbers were mean annual estimates.

Table 2-1. SHORT PERIOD RESONANCES OF THE INNER PLANETS (Explanatory Supplement to the Astronomical Ephemeris, 1961.) (Blizard, 1969)

PERIOD	TROPICAL YEARS
46 Siderial Revolutions of Mercury	11.079
18 Siderial Revolutions of Venus	11.074
(137 Synodic Revolutions of Moon)	(11.077)
11 Siderial Revolutions of Earth	11.000
6 Siderial Revolutions of Mars	11.286

Table 2-2. LONG PERIOD RESONANCES OF THE OUTER PLANETS (Explanatory Supplement to the Astronomical Ephemeris, 1969.) (Blizard, 1969)

PERIOD	TROPICAL YEARS
6 Siderial Revolutions of Saturn	176.746
15 Siderial Revolutions of Jupiter	177.933
9 Synodic Periods, Jupiter - Saturn	178.734
14 Synodic Periods, Jupiter - Neptune	178.923
13 Synodic Periods, Jupiter - Uranus	179.562
5 Synodic Periods, Saturn - Neptune	179.385
4 Synodic Periods, Saturn - Uranus	181.455

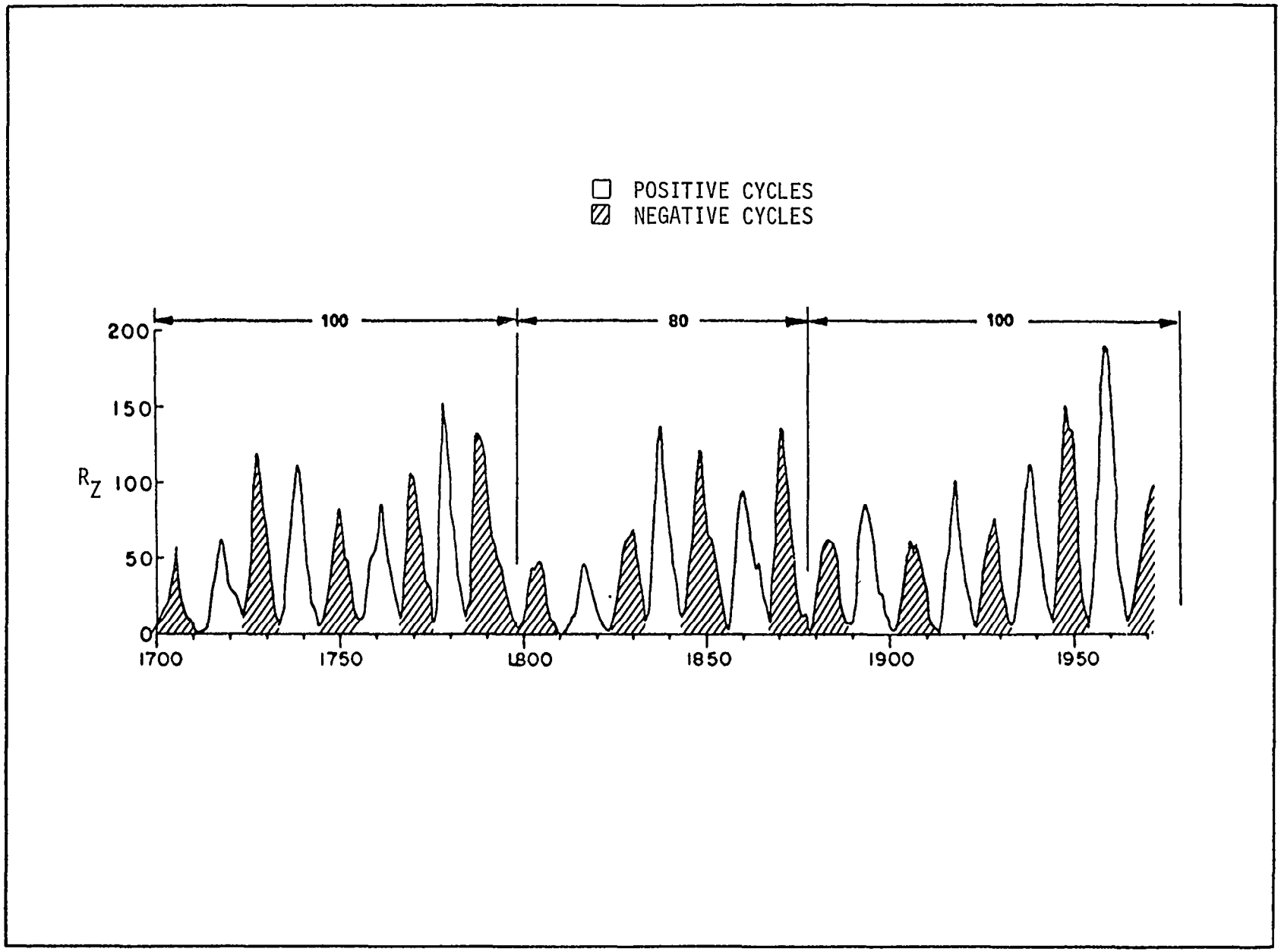

Figure 2-1. ANNUAL SMOOTHED SUNSPOT NUMBERS

Most of the analysis in this paper is based on data for eleven-year cycles 1 - 20. Since these include the data for cycles 1-8 before the Wolf numbers were defined, there has been legitimate doubt as to the reliability of the data from the first set. The statistical evaluation of McNish and Lincoln (1949) and Slutz, et al. (1970) indicated a high probability that the two sets (1-8, 9-19) were from two different populations. However, if the sunspot series has a built-in correlation, the apparent difference in statistical characteristics could be due to the point of division between the sets. This latter question has been studied by dividing the complete set into odd and even cycles. The results of a contingency test yielded a chi square value of 5.2, indicating that the odd and even sets came from the same population (Gray, 1970). The chi square result also indicates that there appears to be no characteristic differences between odd and even cycles, or no simple 22-year cycle characteristics. Similar tests were used subsequently to indicate population differences between positive and negative cycles, as defined later in this report.

In addition to the basic 11-year cycle, the following longer periods have been identified:

- 22-year Hale cycle
- 80- to 100-year Gleissberg cycle
- 180-year Jose cycle.

Of these longer periods, the 180-year period has been the most difficult to establish, due to the relatively short span of reliable solar data available (approximately 220 years). A number of authors have noted the apparent similarity of structure between cycles 1, 2, 3, and 17, 18, 19, separated by approximately 180 years. Both of these sets of cycles have periods shorter than 11 years and peak magnitudes monotonically increasing in height. A more detailed study has been made by Suda (1962) and Jose (1965). Jose's analysis included available data over a period of 360 years. He concluded that the effective period is given by 178.55 ± 1.05 years. This analysis has been confirmed by Portig (1965) and Briér (1970), who "linearize" the sunspot series by using $(R_Z)^{1/2}$ to reduce the variance, and then use an

autocorrelation analysis. All authors point out the close agreement with the 180-year planetary resonance.

Gleissberg (1944) has used a method of smoothing over four cycles to demonstrate a period of 80 - 90 years in duration. Jose has broken the 180-year basic period into two component secular cycles of 80 and 100 years (Figure 2-1 and Table 2-3).

The basis for Jose's choice of component secular cycles is shown in Figure 2-2. In this figure the sunspot data, organized into an approximately alternating positive and negative cycle sequence, are compared with a planetary parameter, the rate of change of the angular momentum of the sun about the center of mass of the sun and the five outer planets. The assignment of the cycle sign for the most recent cycles (15 - 20) is consistent with the 22-year magnetic cycle established by Hale (1908). A cycle is positive if the leading sunspot in a northern hemisphere pair is positive. The corresponding leading spot for a southern hemisphere pair has a negative magnetic polarity. Jose defined the polarity of earlier cycles by the sign of the angular momentum, dp/dt, for the corresponding peak sunspot epoch. Double negative cycles occur at intervals of 80 or 100 years, when a positive value for dp/dt has no corresponding sunspot maximum. The next expected double negative sequence is for cycles 20 and 21.

In this paper, the 180-year period and the 80- or 100-year subperiods are used as the basis for a more detailed statistical analysis of the sunspot time series. The chi square analysis of the statistics for the odd and even cycle series indicated that there were no significant differences between these sets. A corresponding analysis for the positive and negative cycle sets, using Jose's definitions, yielded much higher values of chi square, indicating a population difference for positive and negative cycles (Gray, 1970). The improved error limits obtained by using the smaller positive and negative cycle subsets afford further support for the new cycle classification. The final verification may depend on the validity of the forecast for a negative magnetic cycle 21. Vitinski (1969) has mentioned a high probability for anomalies in previous 22-year cycle sequences.

Table 2-3. SOLAR CYCLE PARAMETERS

CYCLE NO.	SIGN	R_Z(MAX) (smoothed)	PERIOD (years)	SECULAR CYCLE (years)
1	+	86.5	11.2	
2	-	112.5	9.1	~100
3	+	156.5	9.2	
4	-	140.4	13.6	
5	-	45.1	12.4	
6	+	47.7	12.6	
7	-	71.2	10.6	
8	+	145.7	9.8	~80
9	-	128.7	12.2	
10	+	97.0	11.3	
11	-	140.2	11.7	
12	-	74.5	11.3	
13	+	86.1	11.9	
14	-	62.4	9.6	
15	+	105.4	9.9	
16	-	78.1	10.1	~100
17	+	116.7	10.5	
18	-	151.8	10.0	
19	+	199.5	10.6	
20	-	(110.1)	- -	
21	-	- -	- -	

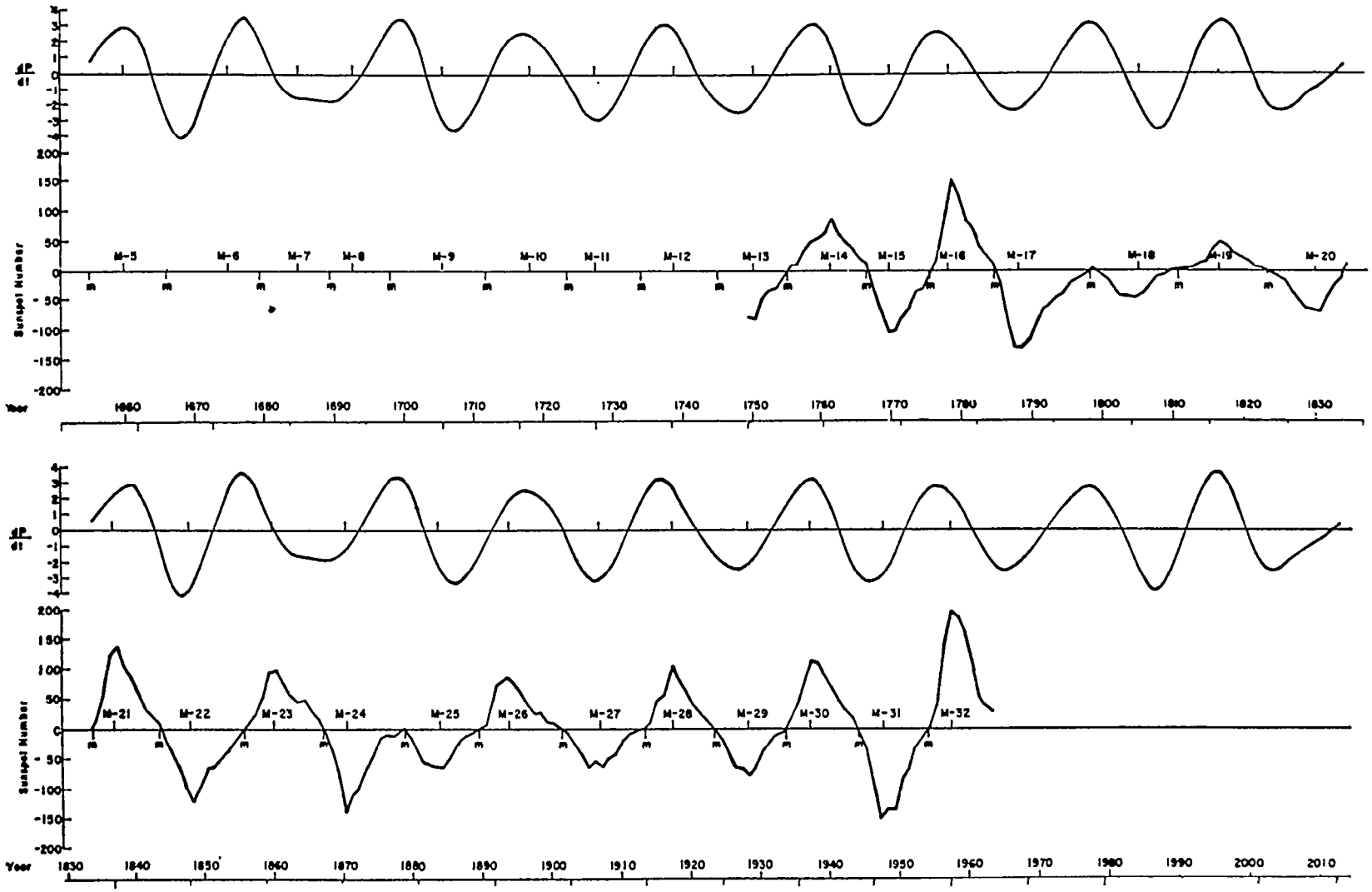

Figure 2-2. dP/dT AND SUNSPOT NUMBER FROM 1655-2012 (AFTER JOSE)

2.3 CLASSIFICATION OF CYCLES

The basic cycle classification to be used is the positive and negative classification established by Jose, Table 2-1. The failure of King-Hele's 80-year secular cycle (1966) in the rise-time behavior is consistent with Jose's cycle assignment. The observation of Dodson and Hedeman (1969) that the number of spotless days for cycle 19 is the least since cycle 10 is consistent with a recent 100-year secular cycle. A similar 100-year extreme in the northern-southern hemisphere spot asymmetry has been found by the same authors.

Current statistical techniques for prediction of future sunspot numbers apply equal weighting to all 19 measured or extrapolated cycles, or to the most recent 12 measured cycles (McNish-Lincoln, 1949), (Weidner, 1969). An objective of the present study is to determine the consequences of the postulated 180-year period and the positive and negative cycle structure.

In this treatment, the 180-year period is assumed fundamental. The current 180-year period includes 16 cycles, 5 through 20. Since the complete data for cycle 20 are not yet available, the data from the last 16 cycles, 4 through 19, will be used as a coherent base for prediction of cycle 20. In this framework, cycle 20 is analogous to cycle 4. The effect of using the 16 cycle base for statistical prediction is to eliminate cycles 1 through 3 from the total data base of cycles 1 through 19.

As noted in Figure 2-1, Jose separates the 180-year period into two component periods of 80 and 100 years. These periods, containing 7 and 9 eleven-year cycles respectively, correspond to the previously indicated secular or Gleissberg cycles. In this classification, there is one more negative than positive cycle in each 80- or 100-year period. Thus, these secular cycles are not commensurate with a 22-year cycle. To date, the total positive set includes cycles 1, 3, 6, 8, 10, 13, 15, 17, and 19. The total negative set includes cycles 2, 4, 5, 7, 9, 11, 12, 14, 16, 18, and 20.

Previous studies have developed a general trend for the peak smoothed sunspot number versus length of cycle (Vitinski, 1962). However, the large standard deviation or low correlation coefficient limited the prediction utility. Figure 2-3 demonstrates the effect of classification of cycles into positive and negative subsets from plots of cycle magnitude versus period. The data are differentiated for the previous 180-year Jose period, cycles 1 through 4, and the current period, cycles 5 through 20. The data tend to fall into two distinct groups or modes of oscillation, I and II. The trends in data are designated by the solid lines for Mode I and Mode II. The two modes are distinguished by two different peak magnitude values for the same cycle period.

For the positive cycles, the Mode I data demonstrate a high degree of coherence and the peak sunspot number is linearly related to period, with a correlation coefficient $r = 0.92$. In this representation, cycle 19 is seen to be anomalously high for its period, and is assumed to belong to a separate Mode II subset. The last two positive cycles, 1 and 3, of the previous Jose period were Mode I oscillations, but the last positive cycle, 19, of the current Jose period was a high magnitude, Mode II oscillation. The difference between Jose cycles may be evidence of a trend with a period greater than 180 years.

The negative cycles fall definitely into two groups or modes, with four representatives in the high magnitude Mode II group. Cycle 2 of the previous Jose period is a Mode I oscillation, whereas cycle 4 is a Mode II oscillation. The slope of the Mode I negative cycle regression relation is much less well defined than for the Mode I positive cycles, and has a smaller magnitude. The character of the Mode II, negative cycle magnitude - period relationship is very poorly defined and will be further analyzed for the individual cycles. The poor definition is largely the result of different degrees of overlap between adjacent sunspot cycles. As discussed later in this report, further analysis indicates a characteristic difference between cycles 11, 18 and 4, 9, designated "typical" and "anomalous." In this framework, negative cycle 20 with a peak magnitude of 110 could be either a high magnitude Mode I

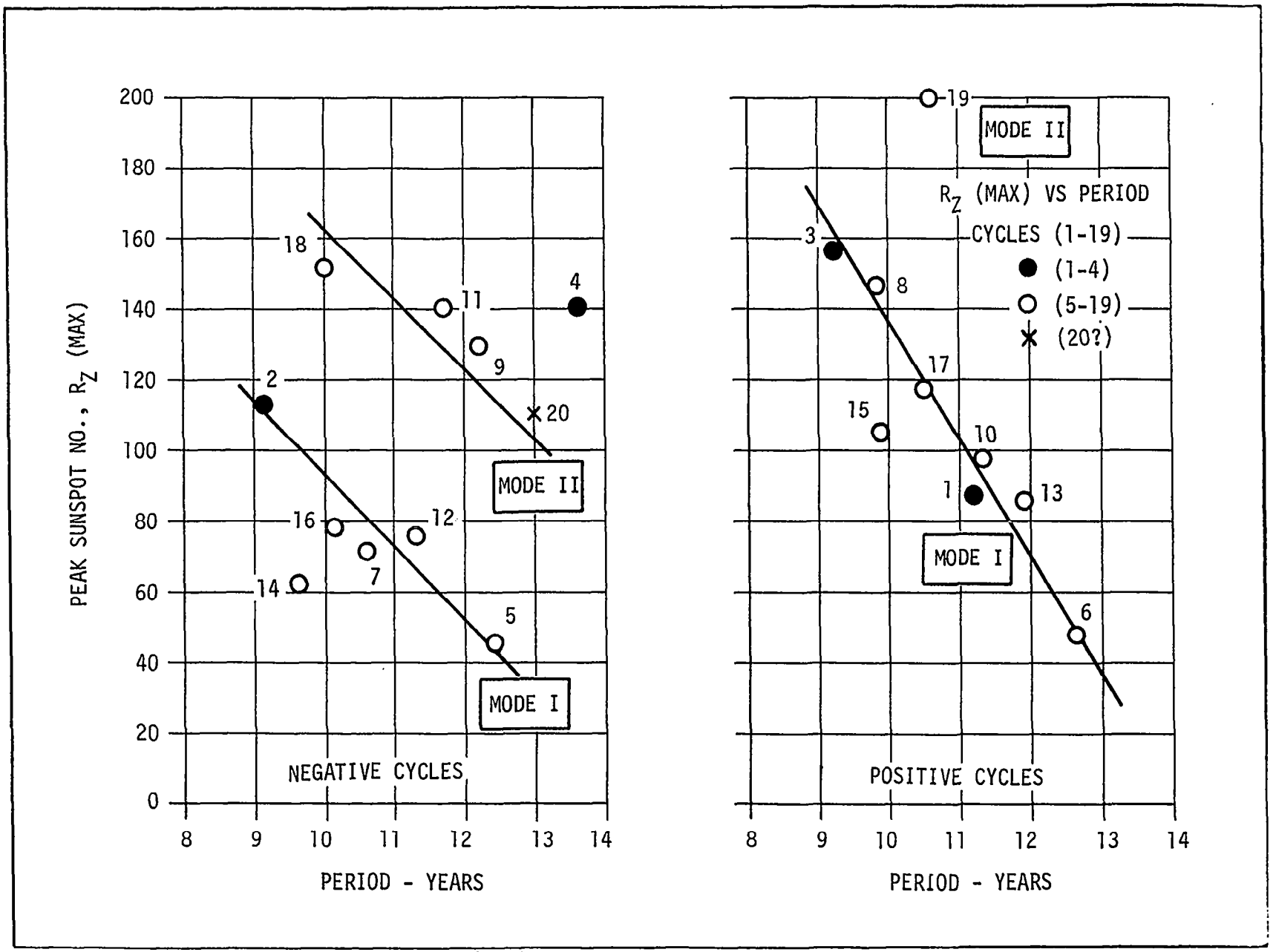

Figure 2-3. R_Z(MAX) VS SOLAR CYCLE PERIOD FOR CYCLES 1 THROUGH 19

oscillation or a low magnitude Mode II oscillation. Further study of the shape and sequence of cycle 20 tentatively identifies it as a Mode II cycle with a period of 13 years.

Figure 2-3 summarizes the peak magnitude-period relationships for positive and negative cycles. Figures 2-4 and 2-5 summarize the sunspot peak magnitude time series for positive and negative cycles. The peak magnitudes are plotted for the epoch of the corresponding preceding minimum. The positive cycle data indicate a possible 180-year cycle in magnitude, but do not appear to demonstrate a simple 80- to 100-year secular cycle. A general 180-year period is indicated for the negative cycle data, and an 80-year subperiod may also be recognized. The current 180-year epoch data for cycles 18 and 20 appear to be advanced in phase by about 1 year, compared with cycles 2 and 4. On this admittedly simple basis, a negative cycle 21 would have a peak value of about $R_Z = 50$. From Figure 2-4, the peak magnitude of cycle 22 could be as low as 50, corresponding to cycle 6, but may be higher.

A unique consequence of the Jose system of positive and negative cycle classification is the prediction of cycle 21 as a negative magnetic cycle. This cycle marks the beginning of a new Gleissberg cycle, and therefore, a negative cycle 21 should follow a negative cycle 20. All previously observed magnetic cycles have alternated polarity since 1908. Consequently, the appearance of a negative cycle 21 would provide strong support for the planetary hypothesis.

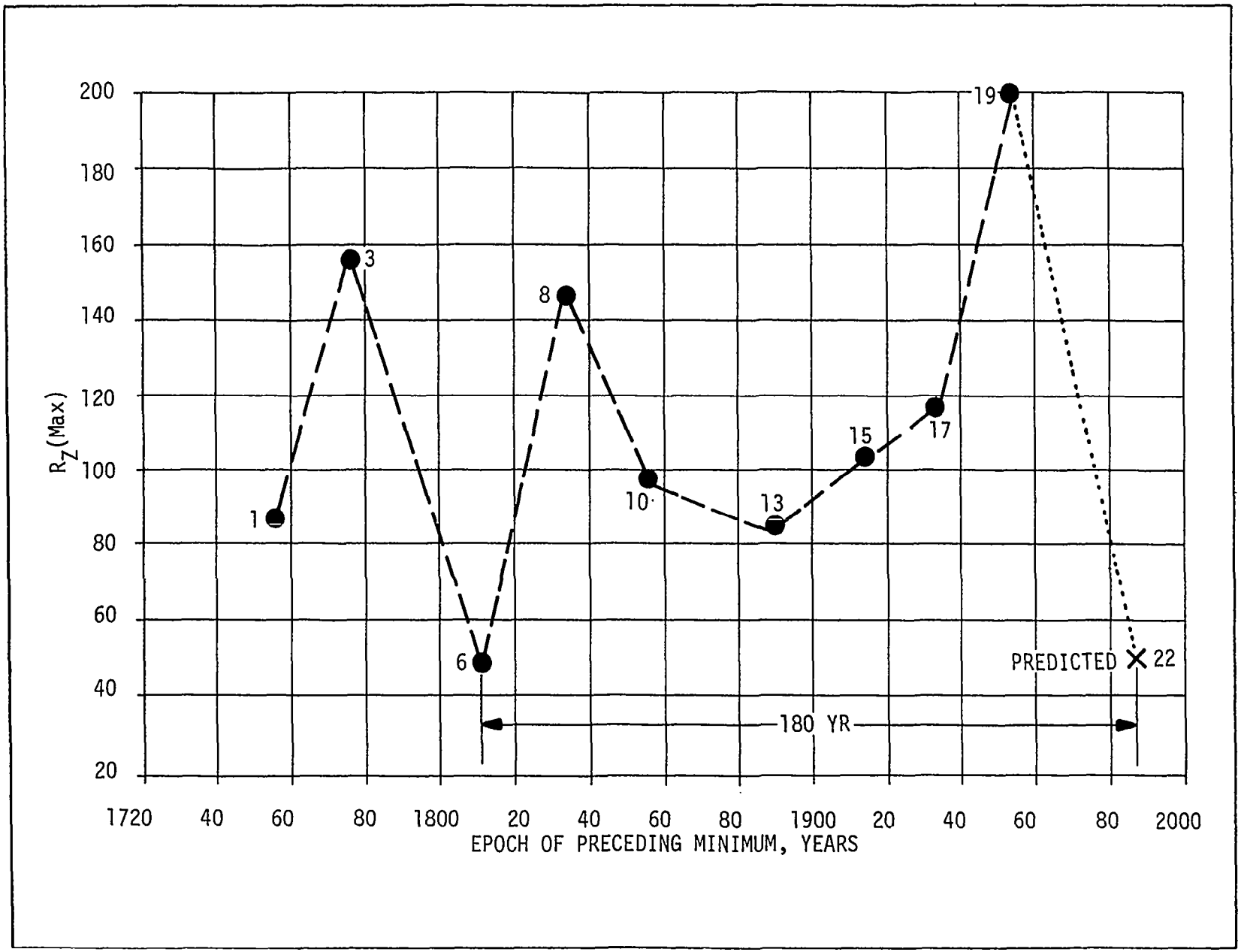

Figure 2-4. TREND OF PEAK MAGNITUDE FOR POSITIVE CYCLES

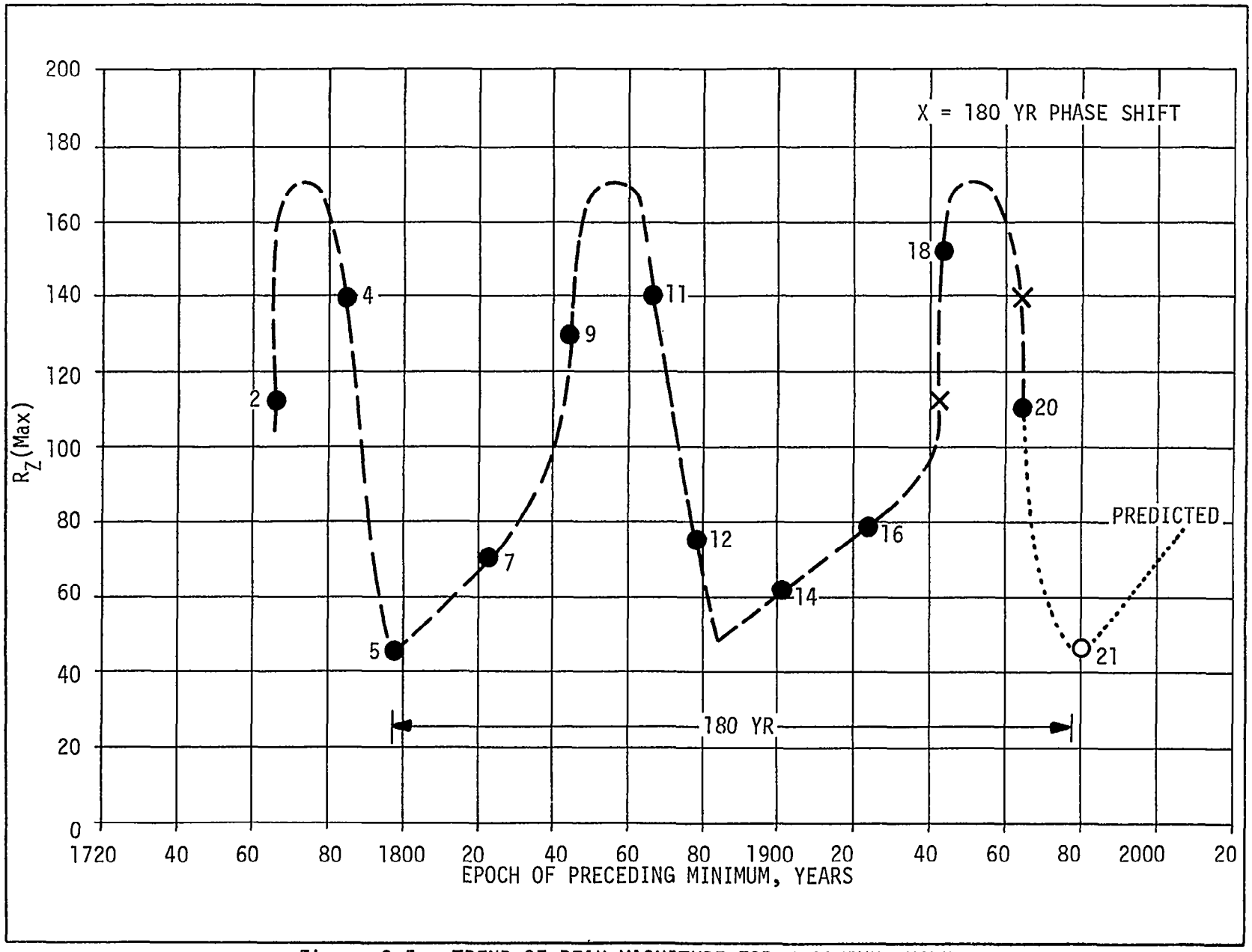

Figure 2-5. TREND OF PEAK MAGNITUDE FOR NEGATIVE CYCLES

Section III

ANALYSIS OF CYCLE CLASSIFICATION

All of the sunspot data presented in this analysis are smoothed annual data, with a running mean evaluated every three months (Weidner, 1969). The mean sunspot number, $\bar{R}_Z$, for a given quarter and a given number of cycles is then evaluated, together with the sample standard deviation S and the 2S confidence limits. If the distribution of the sunspot cycles were strictly Gaussian, the 2S values would represent 95.5 percent confidence limits. Because the distribution is skewed and has a double valued Mode I and Mode II weighting, the Gaussian distribution is not valid. However, the 2S values will be used as an index of statistical tolerance for comparison of different sets of data and for comparison with the conventional Lincoln-McNish statistical model. The above conditions modify the application as confidence limits, but do not affect the principal conclusions with respect to coherent subsets.

The smoothed mean sunspot numbers are evaluated as a function of the phase of the sunspot cycle, normalized to the minimum smoothed value at the beginning of each cycle. The reference curves for $\bar{R}_Z$ versus phase contain the complete data set for cycles 1 through 19. These are compared with the values for 16 cycles (4 through 19), and for positive and negative cycles within the 16-cycle set. The positive and negative cycles are further analyzed for Mode I, Mode II behavior, and cycles of "typical" and "anomalous" duration.

3.1 THE 180-YEAR CYCLE

The shape, magnitude, and 2S limits for cycles 4 through 19 and 1 through 19 are compared in Figure 3-1. The well known characteristic mean shape with a maximum $\bar{R}_Z$ of 96 at 3.75 years after minimum and a 2S value of 95 at the peak is observed for both sets of data. However, for cycles 4 through 19 relative to 1 through 19, the mean length of the effective cycle is increased from 10.25 years to 10.75 years; the $\bar{R}_Z$ value at the minimum is decreased from 16 to 10; and the 2S limit at the minimum is decreased from 19 to 13. These

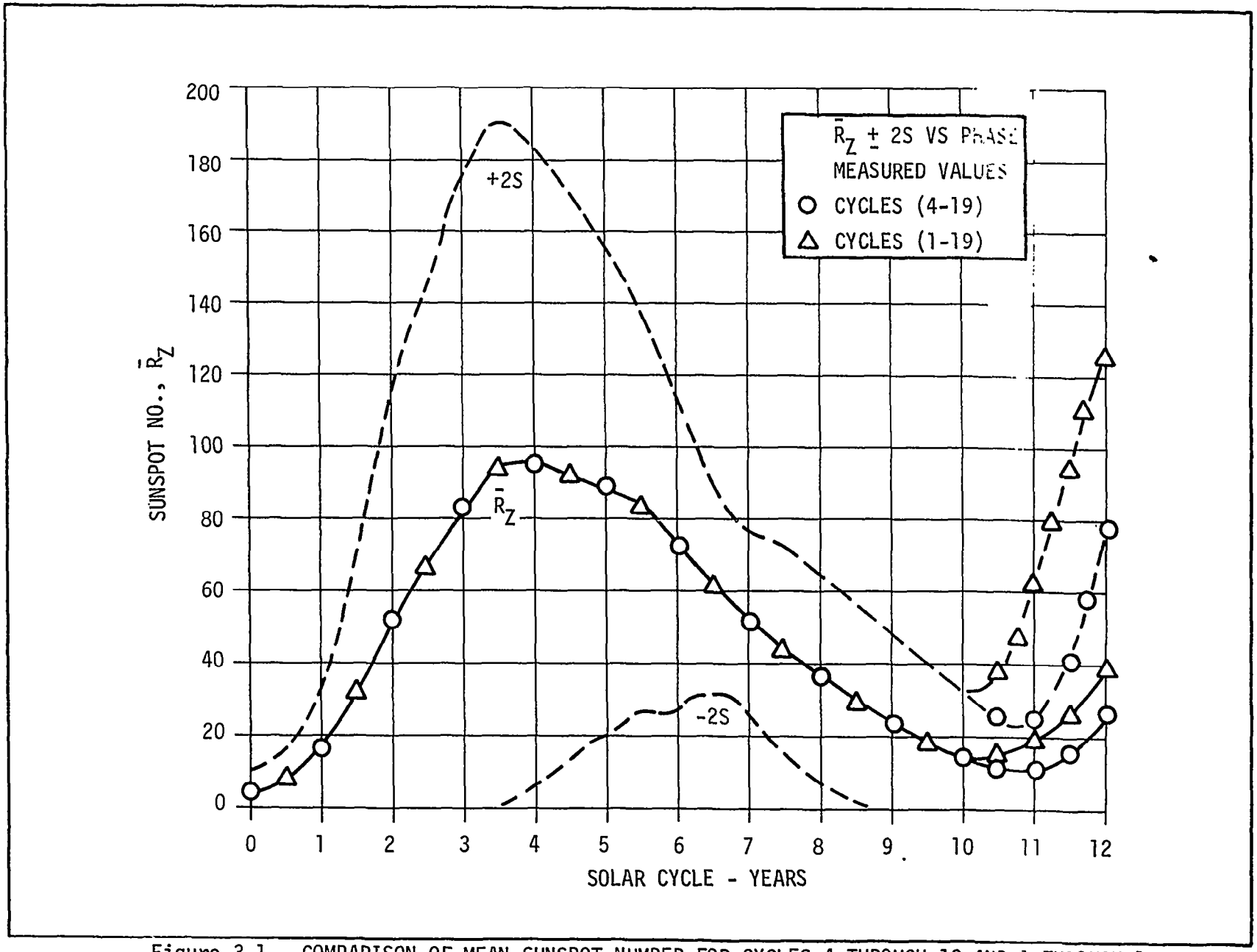

Figure 3-1. COMPARISON OF MEAN SUNSPOT NUMBER FOR CYCLES 4 THROUGH 19 AND 1 THROUGH 19

results demonstrate that the inclusion of cycles 1 through 3 in the data set unduly weights the short cycles, characteristic of the high magnitude Mode I cycles at the end of the previous 180-year Jose period. From this point on, all further analysis is restricted to the 16 cycles, 4 through 19.

3.2 POSITIVE AND NEGATIVE CYCLES

Cycles 4 through 19 are subdivided into a seven-cycle positive set (6, 8, 10, 13, 15, 17, 19) and a nine-cycle negative set (4, 5, 7, 9, 11, 12, 14, 16, 18). Figure 3-2 compares the mean $\bar{R}_Z$ values as a function of cycle phase for these positive and negative sets. The results demonstrate an obvious difference in mean shape and magnitude, and an apparent agreement in mean duration of 10.75 years. The positive cycles have a typical "sawtooth" or triangular shape and negative cycles have a "square wave" or trapezoidal shape. Three and one-half years after the beginning of the cycle, the $\bar{R}_Z$ values are 107 and 87 for positive and negative cycles respectively. The positive cycles have a lower minimum value and a steeper slope than the negative cycles for the first two years. Five years after the origin, the shape for positive and negative cycles is nearly the same. The 2S limits for the positive and negative data sets (Figures 3-3 and 3-4) are the same or smaller than for the complete data set (1 through 19), thus yielding an additional basis for coherence between the smaller data sets. Relative to cycles 1 through 19, there is a noticeable reduction in 2S values 6.5 years after minimum for negative cycles.

3.3 DURATION AND MAGNITUDE OF CYCLES

The results of an analysis of mean cycle lengths, $\bar{\tau}$, and sample standard deviations for various cycle subsets are given in Table 3-1.

Table 3-1 shows that the nine negative cycles have the largest standard deviation in period, compared with the values for all cycles; i.e., 1.25 years versus 1.13 years. A further analysis demonstrates that this is due to two anomalously long cycles of high magnitude, 4 and 9. When these two cycles are eliminated, the typical set of seven negative cycles has a standard deviation of 0.95 years, comparable with that for the seven positive cycles

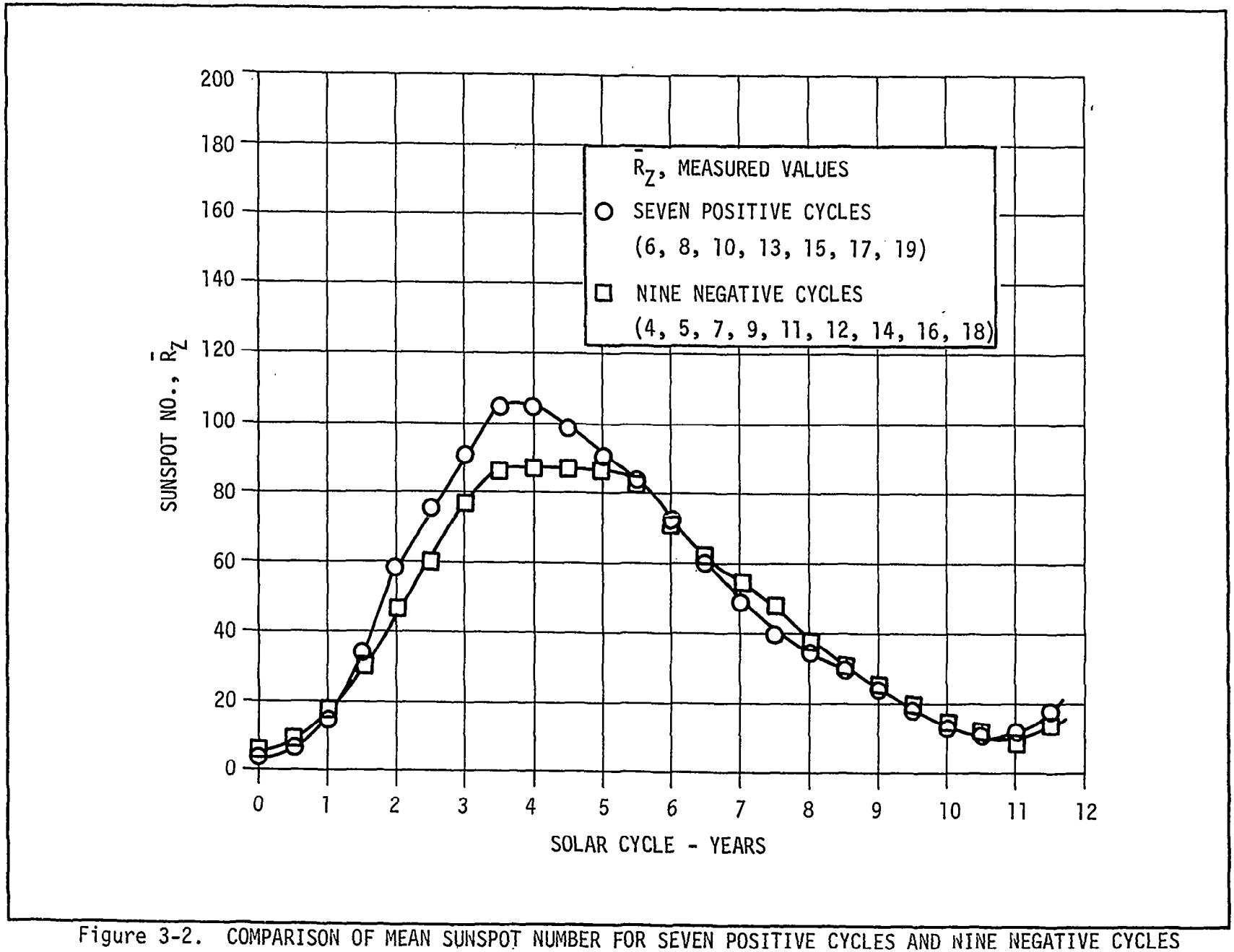

Figure 3-2. COMPARISON OF MEAN SUNSPOT NUMBER FOR SEVEN POSITIVE CYCLES AND NINE NEGATIVE CYCLES

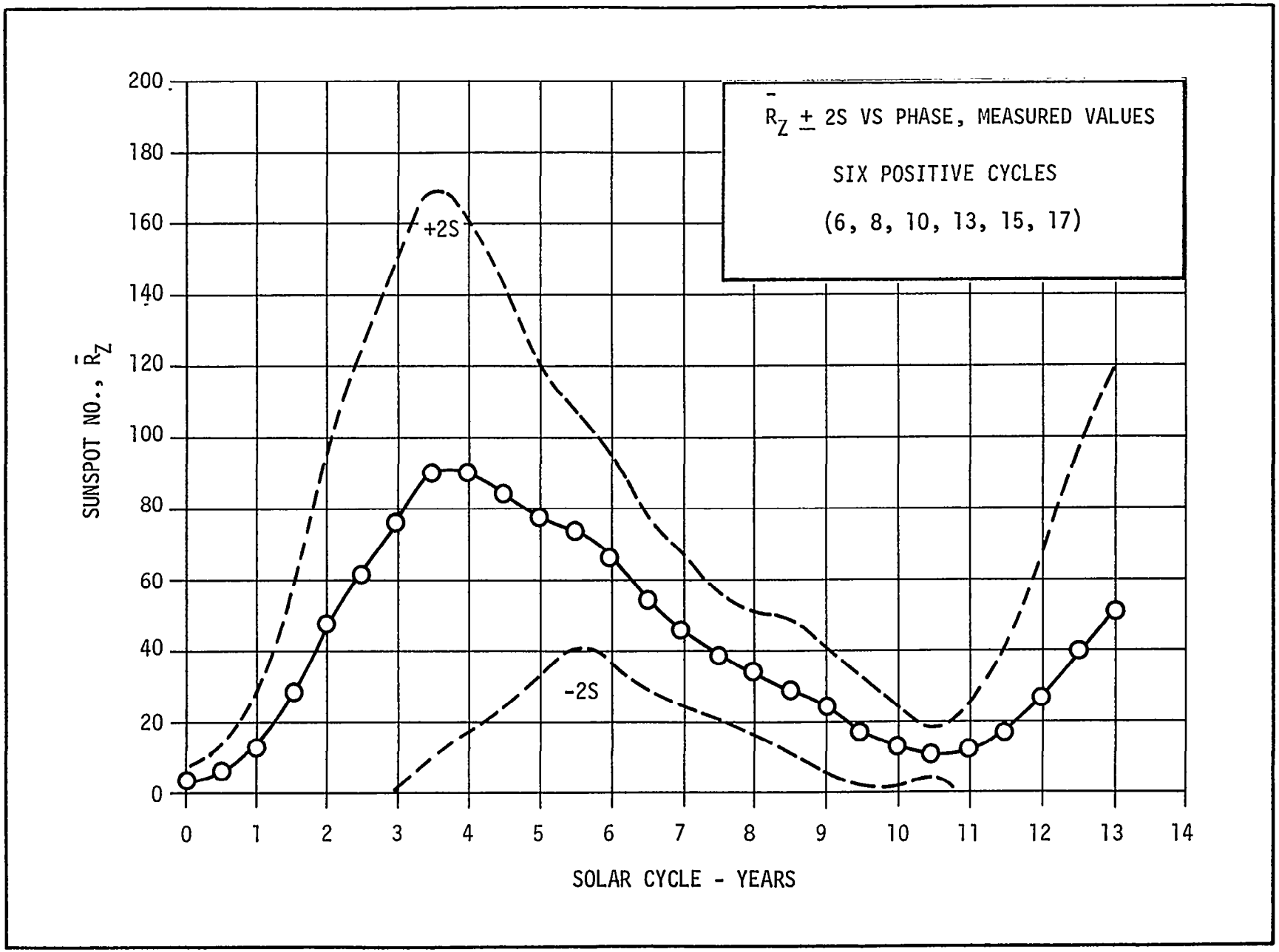

Figure 3-3. MEAN SUNSPOT NUMBER FOR SIX MODE I POSITIVE CYCLES

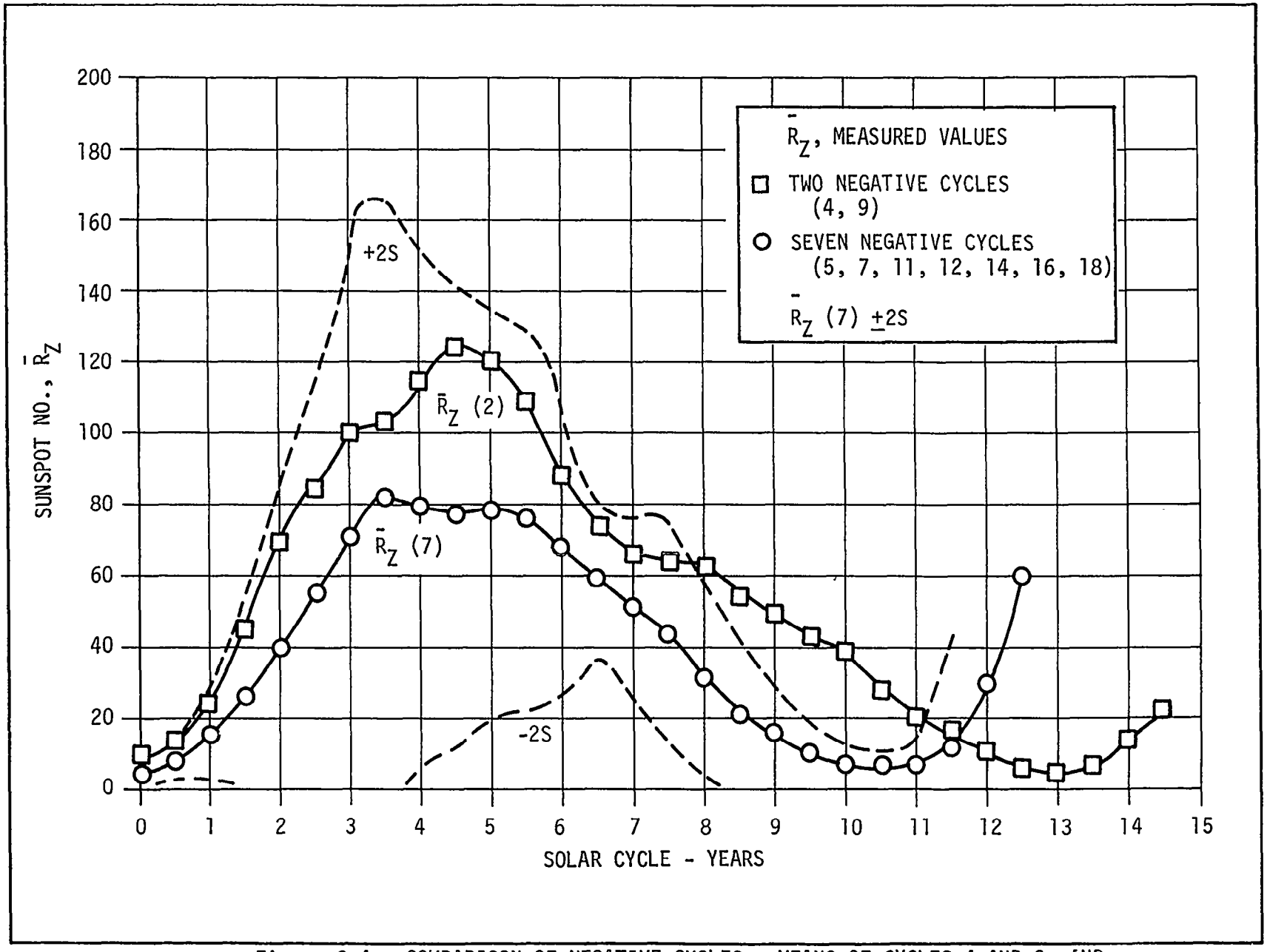

Figure 3-4. COMPARISON OF NEGATIVE CYCLES: MEANS OF CYCLES 4 AND 9, AND SEVEN "TYPICAL" CYCLES

Table 3-1. CYCLE DURATION PARAMETERS

SUBSET	CYCLES	$\bar{\tau}$ (years)	$S(\bar{\tau})$ (years)
19 cycles	1-19	11.02	1.13
16 cycles	4-19	11.13	1.14
7 positive	6, 8, 10, 13, 15, 17, 19	10.94	0.96
6 positive Mode I	6, 8, 10, 13, 15, 17	11.00	1.03
9 negative	4, 5, 7, 9, 11 12, 14, 16, 18	11.28	1.25
7 negative	5, 7, 11, 12, 14, 16, 18	10.81	0.95
2 anom. neg.	4, 9	12.9	

of 0.96 years. A comparison of the means for the two anomalous negative cycles and the seven "typical" negative cycles is shown in detail in Figure 3-4. The $\bar{R}_Z$ values for cycles 4 and 9 are well outside the 2S limits for typical cycles between the cycle phases of 8 and 11 years and the shapes are significantly different. The 2S limits for the seven typical cycles demonstrate a high degree of coherence within the group and define well the last few years of the cycle. The 2S limits are substantially smaller than for the complete set (1 through 19).

Examination of the Mode I and Mode II structure in Figure 2-1 for positive cycles demonstrated the exceptional magnitude of cycle 19. Use of a coherent set of data for prediction purposes requires the elimination of cycle 19 to obtain a "typical" positive set of six cycles. The 2S values for this positive data set are shown in Figure 3-3 and are less in magnitude than for cycles 1 through 19, shown in Figure 3-1. The last 5 years of the cycle are well defined with 2S values of 20 or less. Also, the peak value of $\bar{R}_Z$ is reduced to 91 and the characteristic sawtooth shape is generally preserved.

The shape and magnitude for the selected "typical" sets of six positive and seven negative cycles are compared in Figure 3-5. General shapes are still the same as for the more complete data set (Figure 3-2); but there is a definite difference between sets in shape or magnitude in the region from 8 to 11 years, with the negative cycles having the smaller magnitude. Thus the apparent agreement in shape and magnitude near the minimum shown in Figure 3-2 is due to the effect of the long cycles (4 and 9). Results of this comparison of "typical" cycles also shows that both positive and negative cycles appear to have characteristic peaks at phases of 3.5 years and 5.5 years, with the initial peak more prominent for the positive cycles. This behavior is a further indication of the typical dual peak structure demonstrated by Antalova and Gnevyshev (1965) for both spot area and coronal structure.

3.4 NEGATIVE MODE II CYCLES

According to the proposed system of classification, both cycles 20 and 21 are negative cycles. Cycle 20 is classified negative, as it follows positive cycle 19. Cycle 21 is negative because it initiates another Gleissberg cycle. Since an immediate objective of this study is to provide a basis for improved prediction of cycles 20 and 21, attention is concentrated here on negative cycle characteristics.

With a smoothed peak magnitude of 110, from Figure 2-1, cycle 20 is either a high magnitude Mode I oscillation or a long cycle ($\tau \sim 13$ years) low magnitude, Mode II oscillation. This suggests the possibility of an anomalous cycle 20 with a period of 13 years.

Figure 3-6 compares the mean of the two "typical" Mode II negative cycles (11 and 18) and the two anomalous Mode II cycles (4 and 9). These data are presented together with the 2S limits for the mean of all four Mode II cycles. Cycles 11 and 18 have a typical maximum 3.5 years after the origin and a minimum 10 years after the origin. Evidence of a second peak at 5.5 years is seen. The mean for cycles 4 and 9 has a peak at 4.5 years and a subsidiary peak at 3 years. The differences between typical and anomalous negative cycles make a major difference in the predicted position of the maximum for cycle 21.

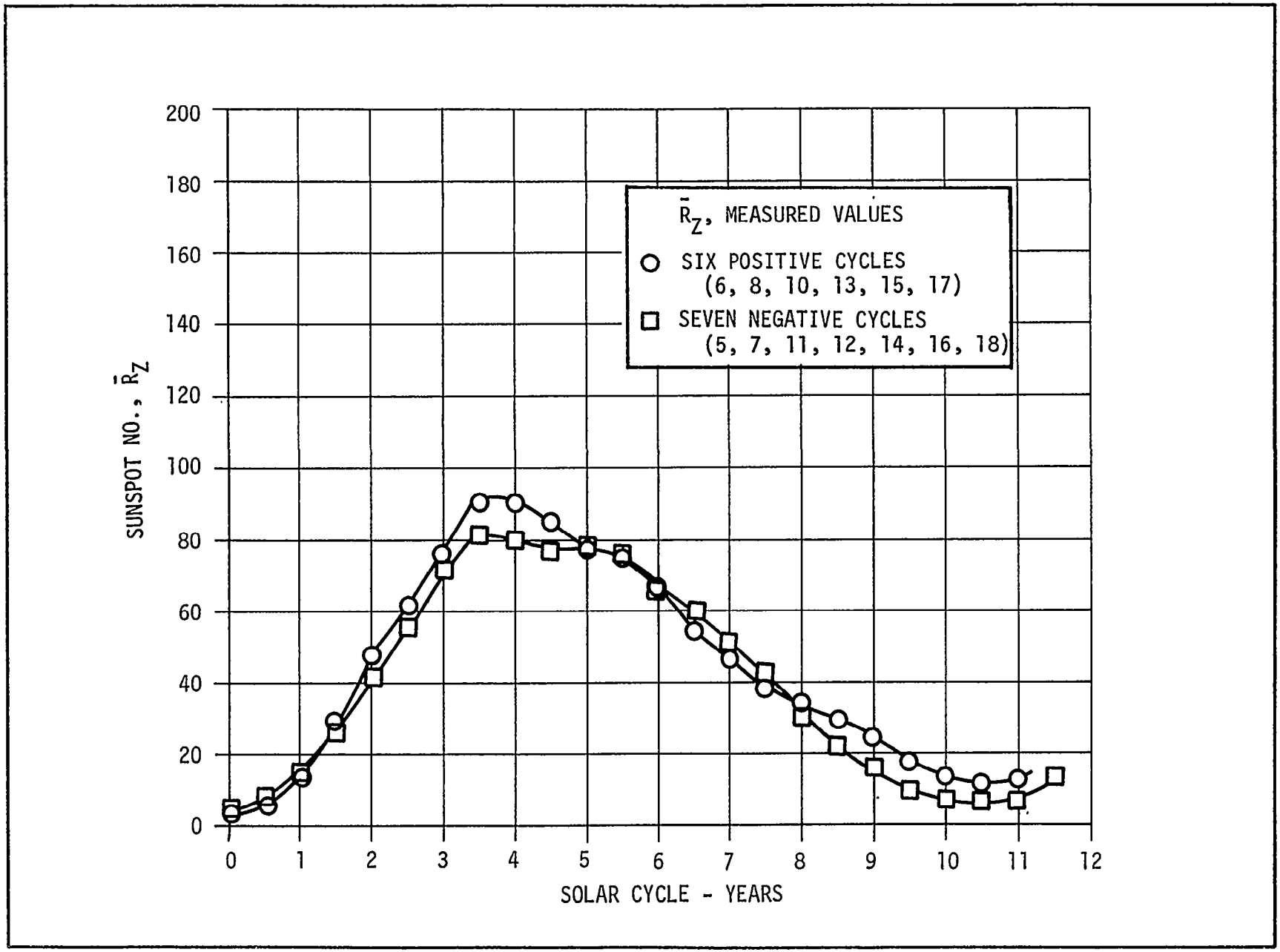

Figure 3-5. COMPARISON OF MEAN SUNSPOT NUMBERS FOR SIX MODE I POSITIVE CYCLES AND SEVEN "TYPICAL" NEGATIVE CYCLES

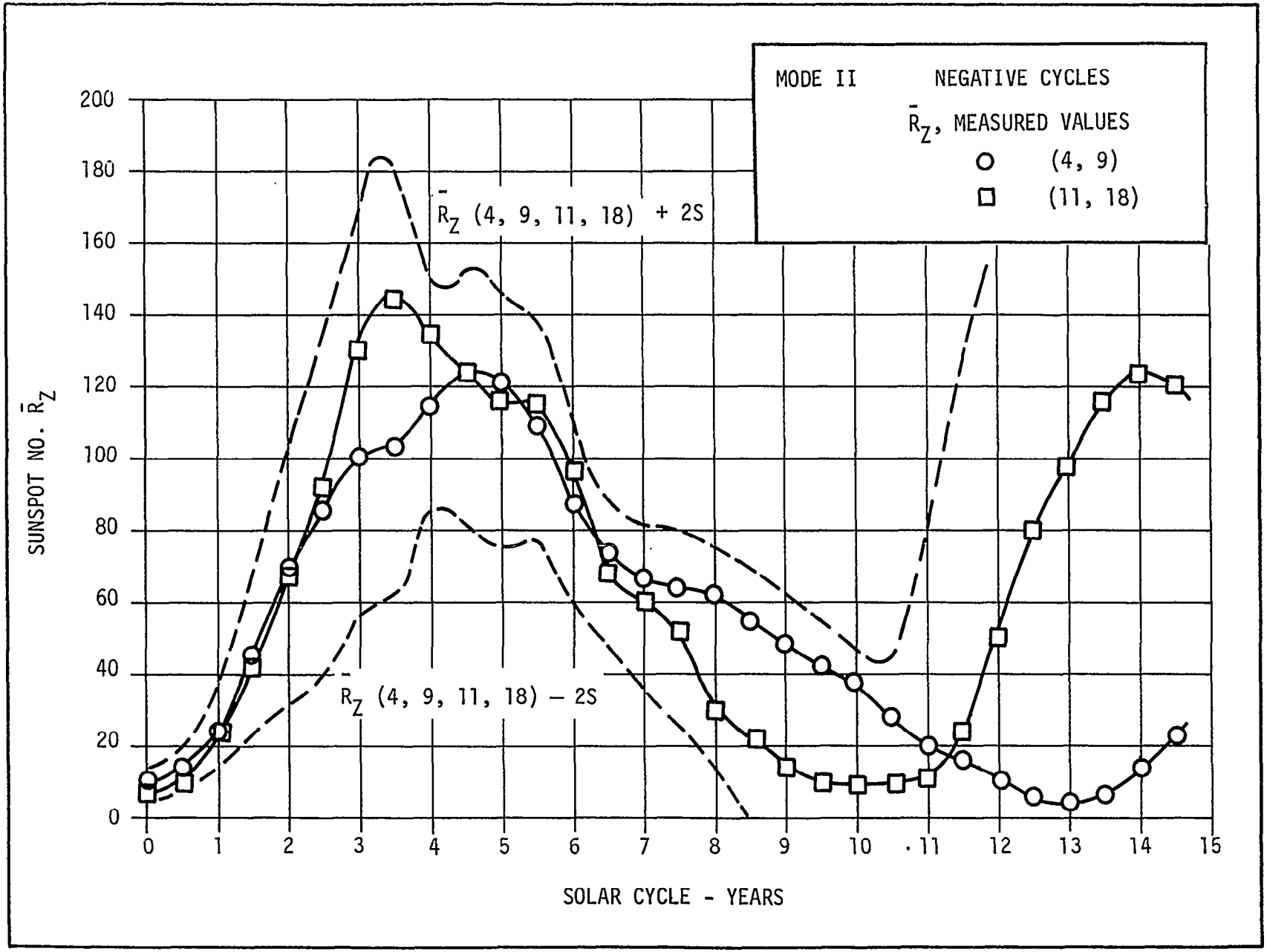

Figure 3-6. COMPARISON OF MODE II NEGATIVE CYCLES: 4 AND 9, AND 11 AND 18

Cycle 20 is compared with each of anomalous cycles 4 and 9 in Figure 3-7. Cycle 20 falls nearly midway between cycles 4 and 9 for about 6 years. The only comparable Mode I cycle, 2, attained a peak value of 112 at 3.5 years after the origin. Cycle 20 attained a peak value of 110 four years after the origin, and therefore is probably a Mode II oscillation. Of four Mode II negative cycles, two are anomalous. This condition suggests a significant probability for cycle 20 to be anomalous. The fact that cycle 20 is the 180-year analog of cycle 4 increases the probability of an anomalous cycle.

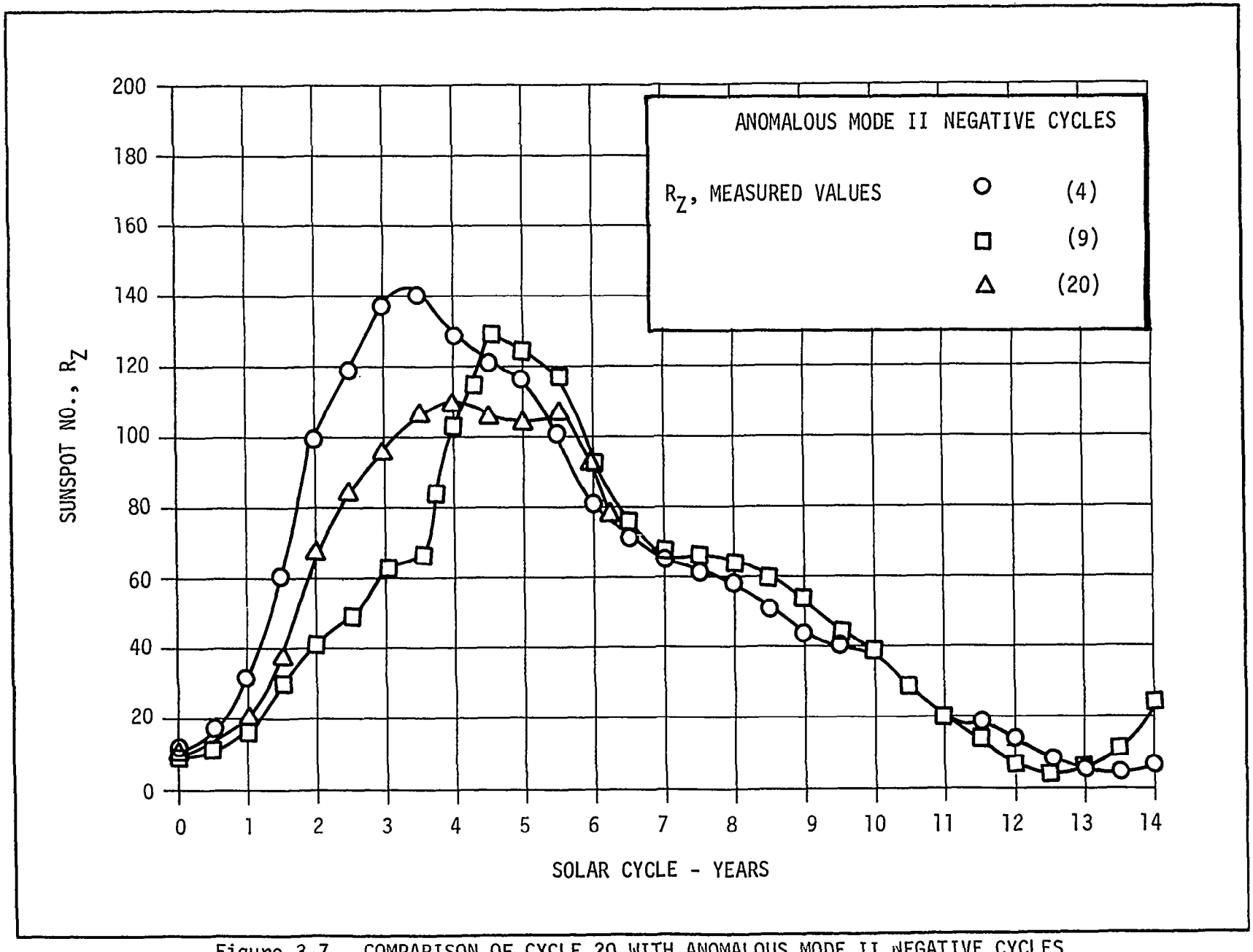

Figure 3-7. COMPARISON OF CYCLE 20 WITH ANOMALOUS MODE II NEGATIVE CYCLES

Section IV

PREDICTIONS FROM THE LINEAR REGRESSION MODEL

The effect of the classification of cycles for the linear regression prediction technique is presented in this section. The effects on the forecasts for cycles 20 and 21 are emphasized. The approach assumes that an estimate of the class for the cycle to be predicted, together with improved statistics for that class, will yield an improved forecast, i.e., a mean value with smaller 2σ limits compared with those for the total data set, (cycles 1 through 19). In forecast evaluation, the "σ" values calculated are rms error estimates, based on the two degrees-of-freedom utilized, i.e., the mean value and a single prediction point. Classification of the anticipated cycle also determines the number of similar previous cycles available as a base for a statistical forecast.

The MSFC Solar Activity Prediction Model (Wiedner, 1969) was used for all the forecasts made in this study. This basic linear regression technique, with its dependence on the mean value of the sunspot number and deviations from the mean for a given phase of the sunspot cycle, was initiated by Lincoln and McNish (1949). The extension from a 1-year forecast to an n-year forecast was developed by Boykin and Richards (1966). The MSFC program uses 60 quarters (15 years) of smoothed data for forecasts beyond the current cycle. Results of the forecast are a function of the cycle set used for a data base (positive or negative, Mode I or Mode II, typical or anomalous) and of the sunspot number for the last experimental point used for the prediction. Experience with the model forecasts demonstrates that the prediction for an epoch of greater than 7 years depends on the deviation of the prediction point from the mean and the cycle subset used as a data base. For the complete data base (1 through 19), $\bar{R}_Z$ approaches the mean value at the end of the cycle. For the typical positive cycle data base, the deviation from the mean at the end of the cycle is negatively correlated with the deviation near the beginning. For the total negative cycle data base, the deviation from the mean at the end of the cycle is positively correlated with the deviation near the beginning.

These conditions mean that more information is available and can be utilized for cycle shape prediction.

4.1 NEGATIVE CYCLE 20 FORECASTS

The experimental data (26 quarters) for cycle 20 are compared with fourth quarter forecasts for a data base of all cycles (1 through 19) in Figure 4-1 and for the nine negative cycles in Figure 4-2. Results indicate maximum $\bar{R}_Z$ deviations from the forecast of about the same magnitude for both data bases. However, the shape of the forecast is appreciably different for the two cases, and the data agree better with the forecast from the negative cycles. Both the mean value and the standard deviation at the 11-year minimum are reduced using the negative cycle forecast, relative to the total data base. Two additional benefits for the negative cycle data base are the reduced rms error estimate at the maximum and, especially, 6.5 years after the origin.

Forecasts from the 19th quarter for a data base of cycles 1 through 19 and nine negative cycles are compared in Figures 4-3 and 4-4. The 2σ rms error estimates from the interval 4.75 years to 6.25 years are reduced for the nine negative cycles by nearly a factor of two, compared with those for the total data base. The 2σ values are nearly the same from 7.5 years to 10 years and considerably less at the minimum for the negative cycle forecast. The 2σ values of ± 30 beyond 8 years are due principally to the effect of anomalous cycles 4 and 9. The small error estimate at the 11-year "minimum" demonstrates the effect of anomalous cycles 4 and 9 on the forecast, and indicates that after 7 years the mean value may not be a good estimate of the cycle due to a bi-modal distribution. The independent evidence noted above for a probable anomalous cycle 20 emphasizes this condition. The results demonstrate the bi-stable option for the minimum at a phase of about 10.5 years or at about 13 years.

4.2 TYPICAL AND ANOMALOUS CYCLE 20 AND 21 FORECASTS

The effect of further refinement of the forecast for cycles 20 and 21 is shown in Figures 4-5 and 4-6. It is assumed that both cycles 20 and 21 are

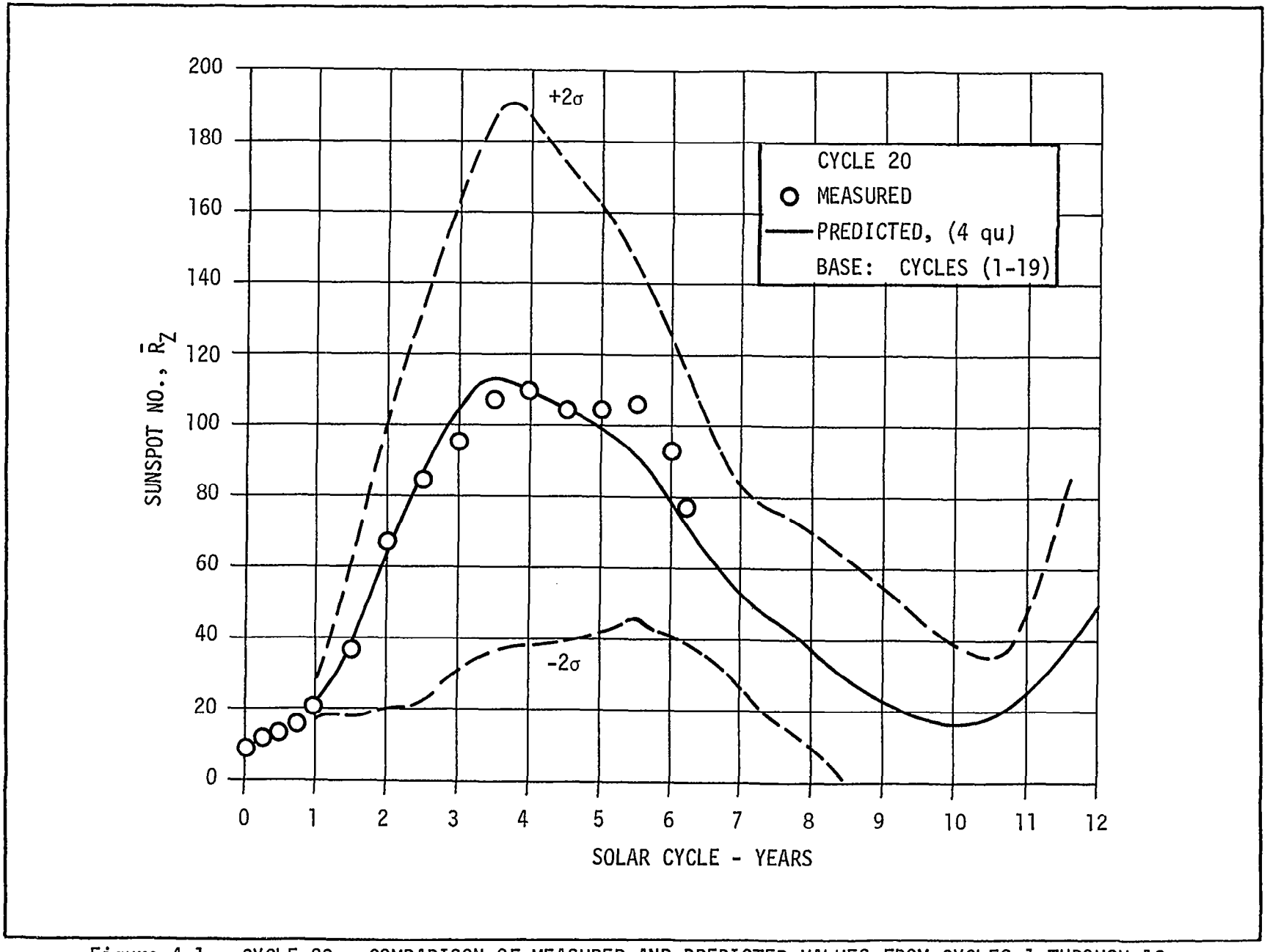

Figure 4-1. CYCLE 20: COMPARISON OF MEASURED AND PREDICTED VALUES FROM CYCLES 1 THROUGH 19

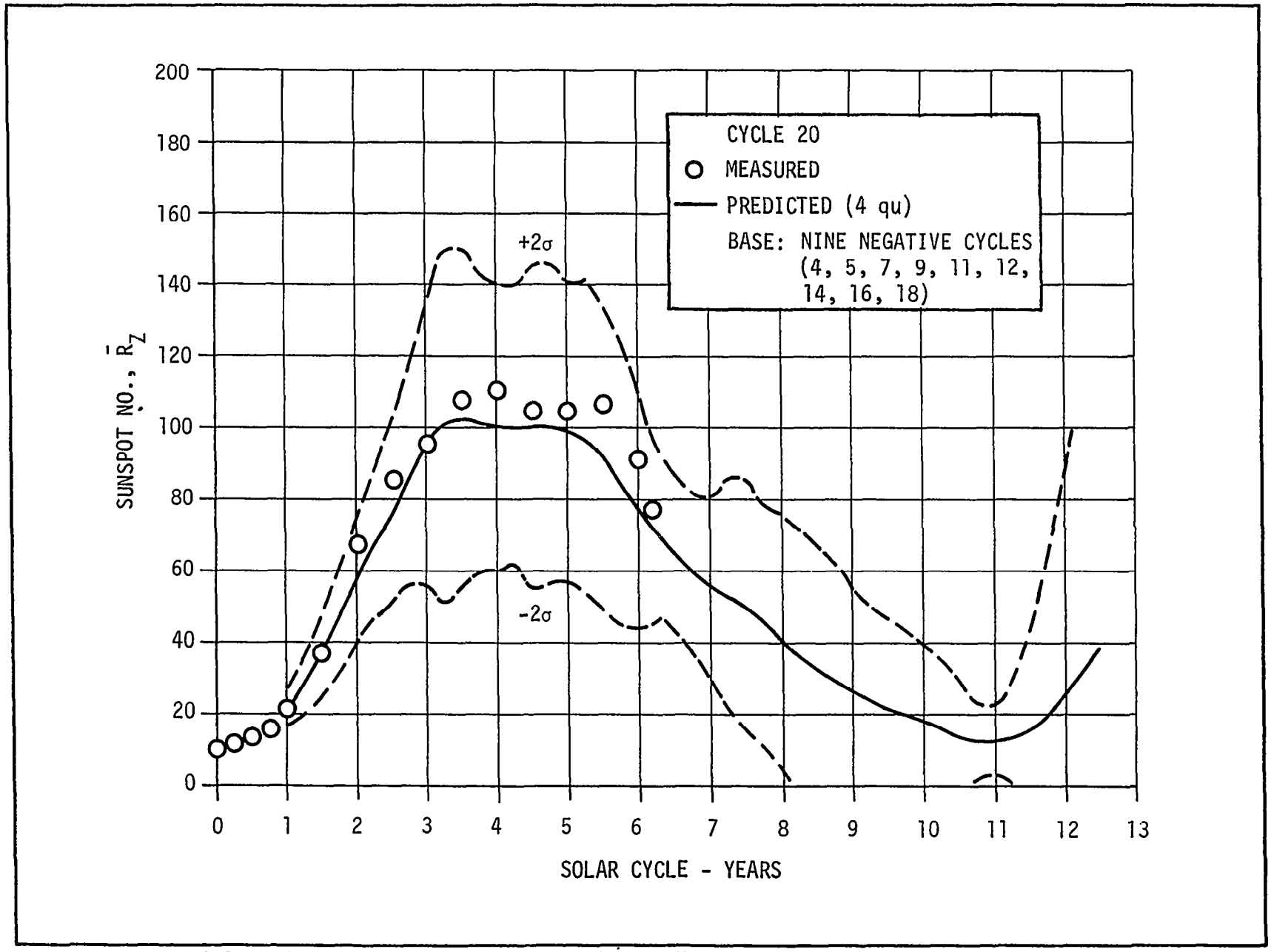

Figure 4-2. CYCLE 20: COMPARISON OF MEASURED AND PREDICTED VALUES FROM NINE NEGATIVE CYCLES

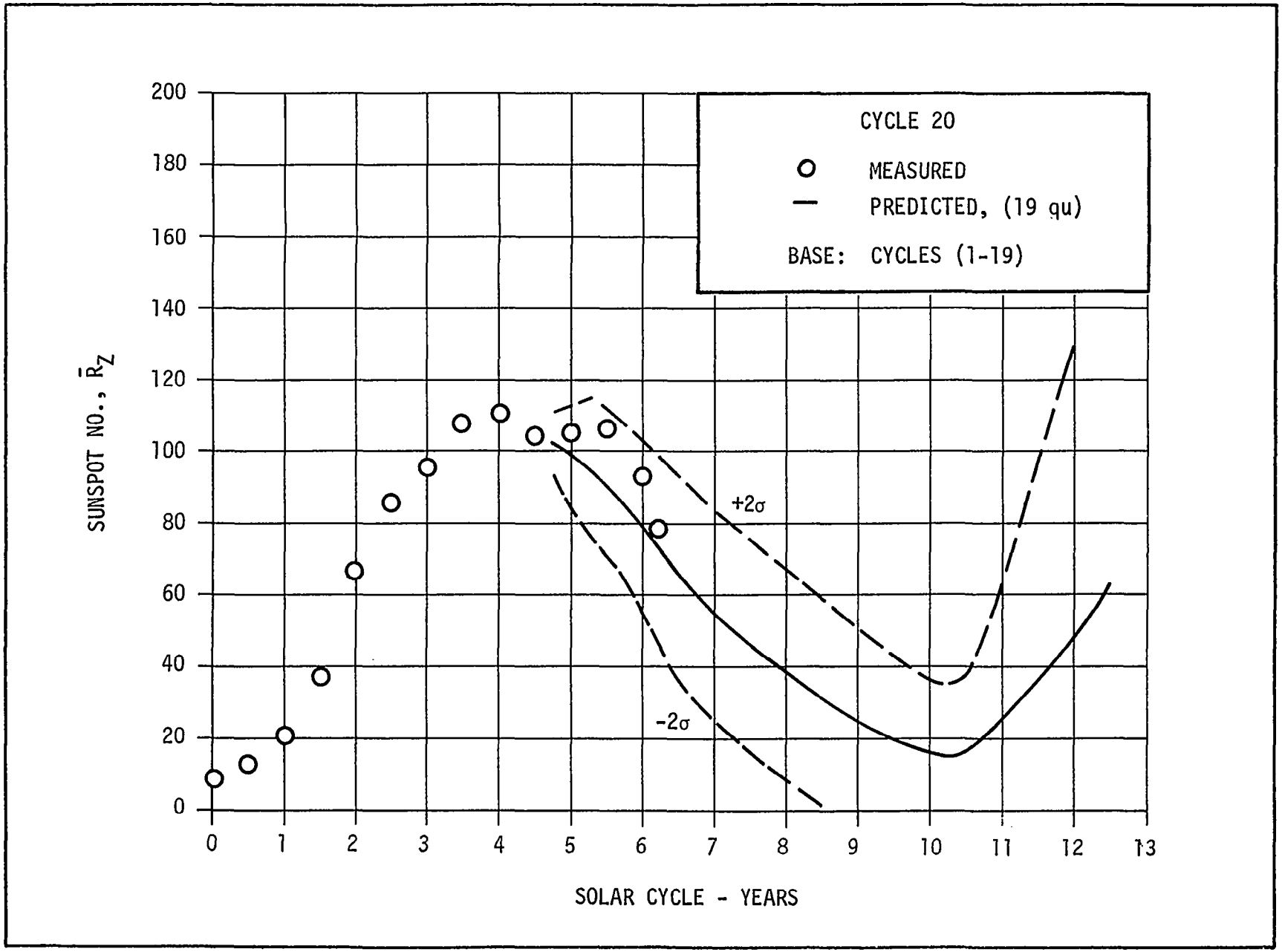

Figure 4-3. BALANCE OF CYCLE 20, PREDICTED VALUES FROM CYCLES 1 THROUGH 19

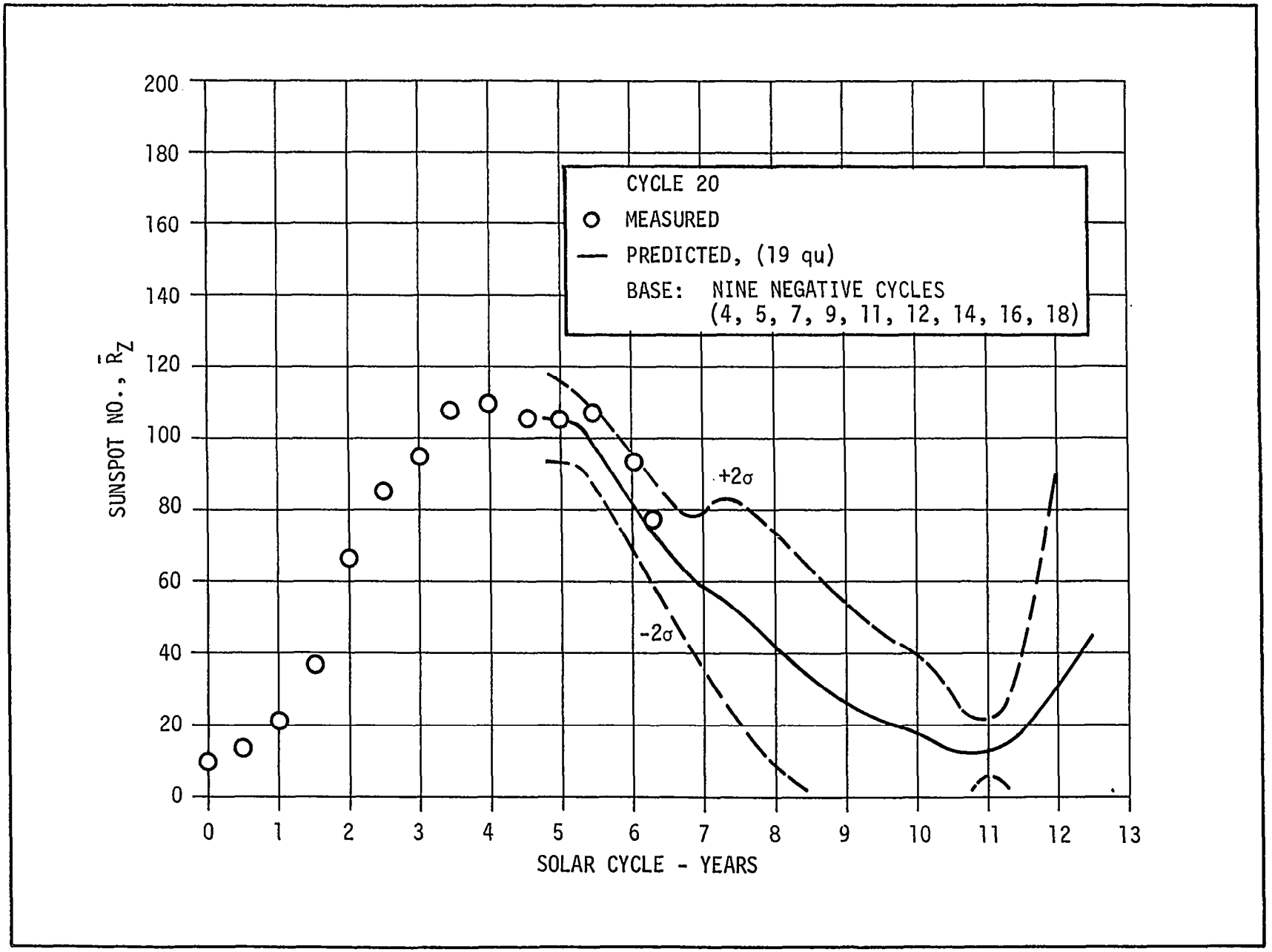

Figure 4-4. BALANCE OF CYCLE 20, PREDICTED VALUES FROM NINE NEGATIVE CYCLES

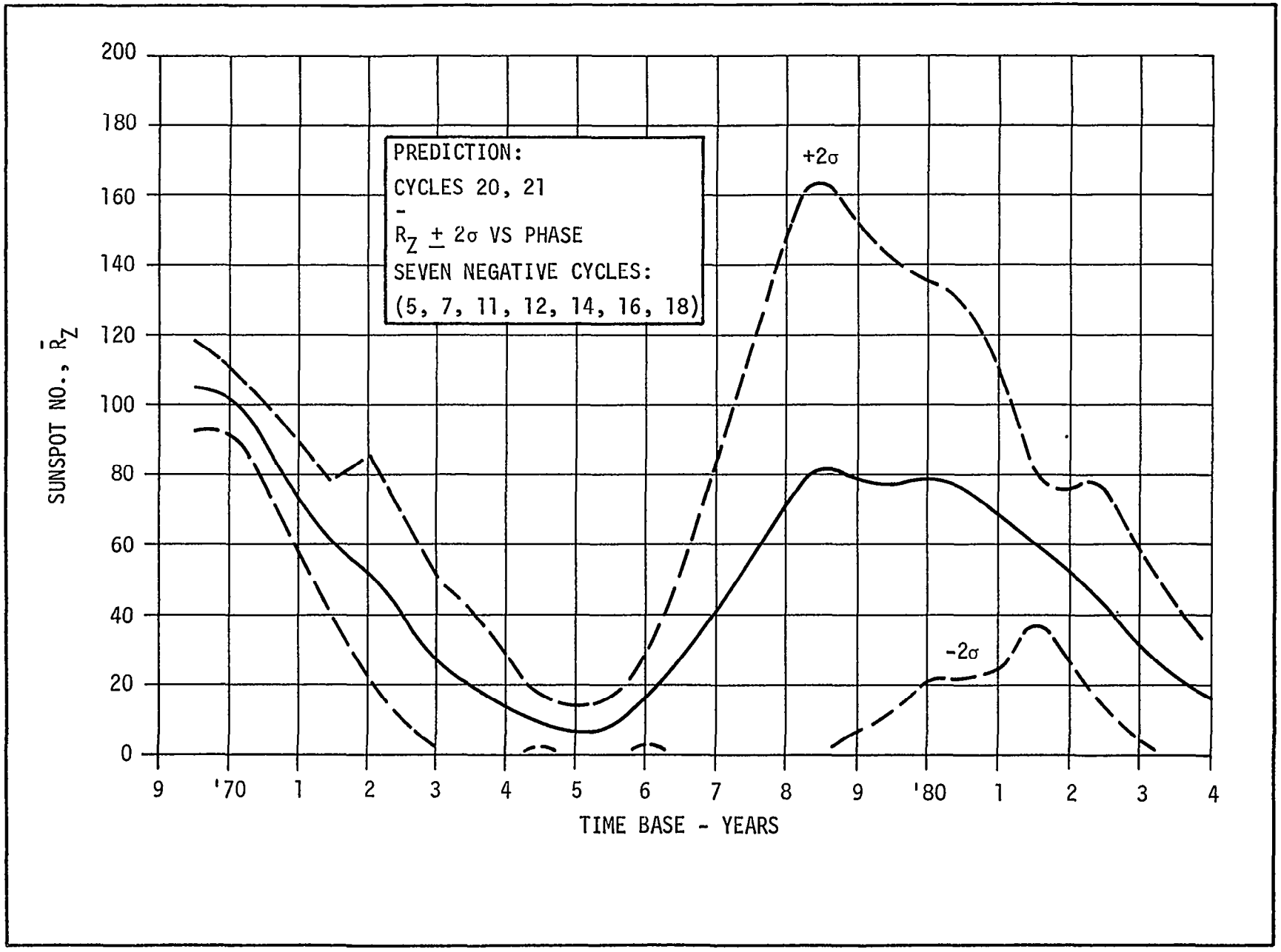

Figure 4-5. PREDICTION OF CYCLES 20 AND 21 BASED ON SEVEN "TYPICAL" NEGATIVE CYCLES

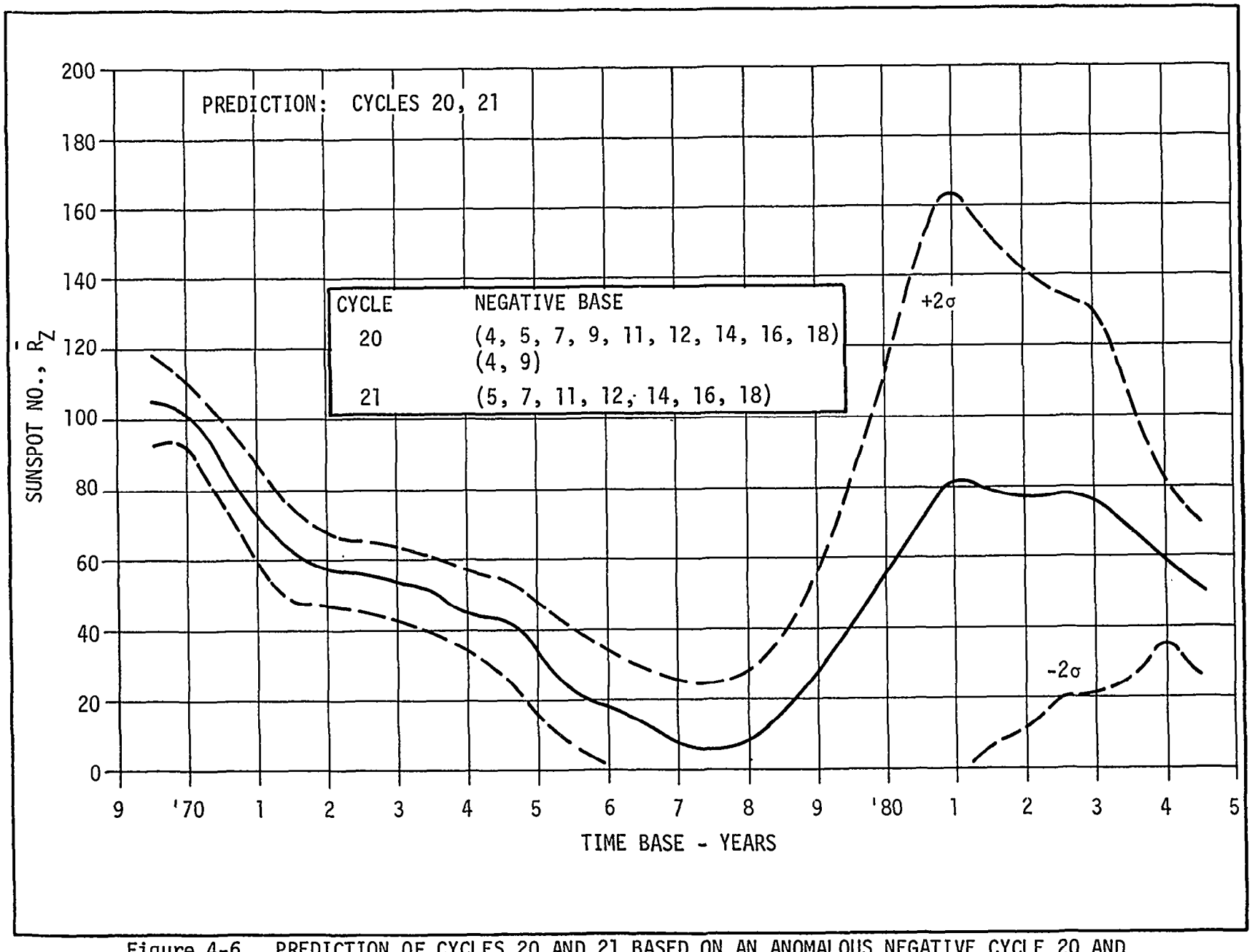

Figure 4-6. PREDICTION OF CYCLES 20 AND 21 BASED ON AN ANOMALOUS NEGATIVE CYCLE 20 AND "TYPICAL" NEGATIVE CYCLE 21

negative and that cycle 21 is not an anomalous Mode II oscillation. This assumption is based on the observation that the anomalous cycles in the past have occurred at or before the end of the corresponding Gleissberg cycle. Thus the estimate for cycle 21 uses data for only the seven "typical" negative cycles (5, 7, 11, 12, 14, 16, 18), both Mode I and Mode II. A less conservative estimate would have included only Mode I cycles, possibly characteristic of the beginning of a Gleissberg cycle. Both of the cycle 20 estimates evaluated have small values for $\bar{R}_Z$ minimum and 2σ estimates, so that the cycle 21 mean $\bar{R}_Z$ estimate can be "patched" directly on to the cycle 20 forecast without the large uncertainty inherent in the total data base (1 through 19).

The cycle 20 forecast in Figure 4-5 is based on the assumption that cycle 20 may be a Mode I or Mode II oscillation and a member of the "typical" negative cycle set. The consequences of this option are seen to be a minimum $\bar{R}_Z$ value in 1975, with significantly reduced mean value and 2σ limits. The maximum uncertainty is at the beginning of 1972, with a 2σ value of about 30. The initial peak value for cycle 21 on this basis is in 1978, and the center-of-gravity of this cycle is in 1979. These characteristics are very similar to predictions for cycle 21 based on the complete data set (Wiedner, 1969) except for smaller 2σ values.

The cycle 20 forecast in Figure 4-6 is based on the assumption that cycle 20 is an anomalous Mode II negative cycle. Since there are only two members in this class, 4 and 9, no statistical forecast is possible due to the two degrees-of-freedom used in the model. Therefore the forecast in Figure 4-6 represents an educated estimate for the mean $\bar{R}_Z$ value and the 2σ values, based on patching of data from 1969.5 to 1971.5 using a base of all negative cycles, from 1971.5 to 1977.5 using a base of cycles 4 and 9, and from 1977.5 on using typical negative cycles. The 2σ values are assumed to be smoothly and slowly increasing values from 1969.5 to 1979. The general behavior is based on the comparison of cycles 4 and 9, and 11 and 18 in Figure 3-6. This estimate places the next minimum in 1977 and the next initial maximum in early 1981, with the center-of-gravity in early 1982. The

results indicate a shift of the $\bar{R}_Z$ mean of cycle 21 by 2.5 years relative to the estimate based on cycles 1 through 19.

This anomalous behavior for cycle 20 is consistent with predictions by Bezrukova (1962), Bonov (1968), Wood (1968), Suda (1962) and Jose (1965).

Section V

IMPLICATIONS OF THE PRESENT STUDY

5.1 GENERAL

The analysis as presented depends upon the presence of planetary orbital resonances which are reflected in the sunspot time series. The results lead to evidence for bi-stable oscillation modes of the sun. One of the most important consequences of the analysis is support for the hypothesis of a negative magnetic cycle 21. This situation has potentially significant consequences for the magnetic characteristics of the balance of cycle 20, and for the requirements for a better physical model for the solar cycle. A model requiring long period asymmetric variations, magnetic dipole structure, magnetic quadrupole structure, rigid rotating core, differential lattitude surface rotation, and coupling with planetary positions or motions seems indicated.

5.2 BI-STABLE OSCILLATION MODES OF THE SUN

The Hale 22-year cycle of positive and negative magnetic structure establishes one pair of bi-stable modes of solar oscillation. Using the observed 80- and 180-year cycles in the sunspot time series, the positive and negative structure of the cycles may be determined back to cycle 1 and ahead to cycle 21. The positive-negative cycle structure assigned by Jose is supported by the independent statistical analysis in this paper and agrees with 22-year cycle anomalies previously studied by Kopecky (1950).

On the basis of the postulated positive-negative structure in the time series, evidence is obtained for a Mode I-Mode II peak magnitude bi-stable structure. Positive cycles provide only a single instance of high magnitude, Mode II oscillation (cycle 19). Negative cycles provide five examples of Mode I oscillation and four examples of Mode II oscillation. There may be some threshold phenomenon that determines which mode a given cycle will follow. It is possible that there are examples of a third mode in the earlier history of sunspot cycles. Finally, there is evidence for anomalously long cycles, with excess activity compared with that observed for typical cycles.

Use of the assumed bi-stable oscillation states to separate the time series into cycles with common characteristics yields significantly improved statistics for prediction purposes. This is a major objective of this report. The results are analogous to studying meteorological time series by separating the data according to common seasons.

5.3 MAGNETIC CYCLE STRUCTURE

The development of a theory for the solar cycle has been based primarily on the Babcock magnetic dipole topological model. This model accounts for the simple alternation of positive and negative sunspot magnetic cycles observed since 1908. This model also agrees generally with Spoerer's law and Maunder's butterfly diagram. However, it does not account for long-period variations of approximately 80 or 180 years in height, duration, and symmetry, or the magnetic quadrupole structure observed at sunspot maximum when the di-polar fields are reversing sign. It definitely does not account for the postulated negative--negative magnetic cycle sequence, or the dual peak character of the latitude structure studied by Antalova and Gnevyshev (1965). Finally, it does not account for the 27.0-day period rigid rotating component of the sun's magnetic field (Severny et al., 1969 and Wilcox et al., 1970).

Sheeley (1964) has studied polar faculae as a function of the phase of the solar cycle (Figure 5-1). The polar faculae are related to the sign and phase of the polar magnetic fields. The results demonstrate that the polar magnetic fields reverse near sunspot maximum, and are 180 degrees out of phase with the sunspot number. If we postulate, according to the Babcock model, that the magnetic structure of a new solar cycle depends upon the structure of the sun's polar magnetic field near the previous sunspot maximum, then a negative north magnetic pole appearing at solar maximum will be followed by a negative sunspot cycle near sunspot minimum. This implies that if cycle 21 is to be a negative magnetic cycle, the polar magnetic field structure will <u>not</u> change at solar maximum for cycle 20, or it will change <u>twice</u> before the end of cycle 20.

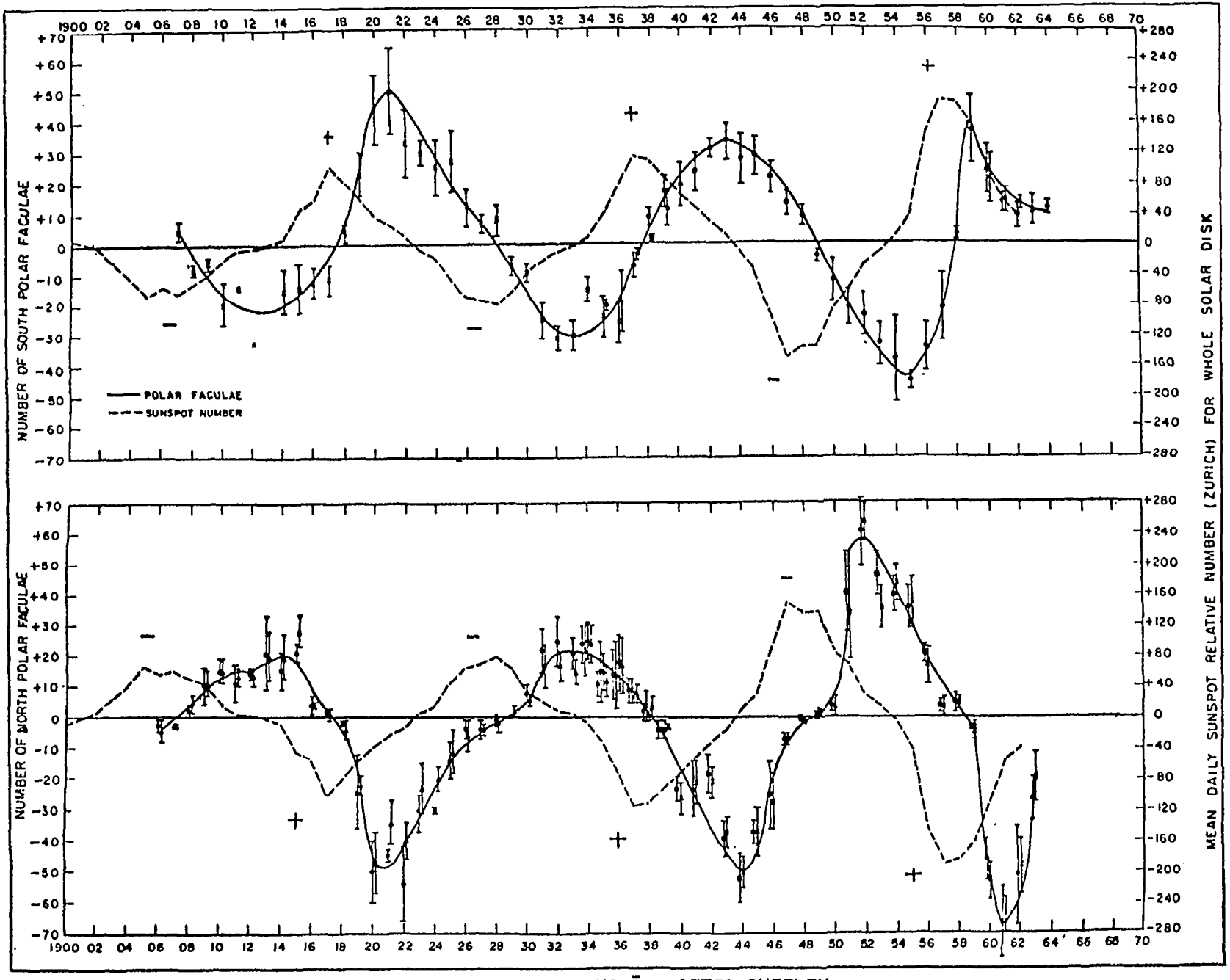

Figure 5-1. POLAR FACULAE VS $\bar{R}_Z$, AFTER SHEELEY

The polar fields have been small for several years and there has not been a definitive polar field reversal as of September 1970 (Howard, 1971). Stenflo (1970) determined that as late as August 1968, the mean latitudes for solar magnetic field sign reversal were 70 and 55 degrees for the northern and southern hemispheres, respectively. Howard (1972) has indicated that according to measurements in 1971, the sun's polar magnetic structure changed from two negative poles to two positive poles. That is, currently the sun is a magnetic quadrupole with two positive poles, with the same structure as at the maximum of cycle 19. The further study of these polar fields may give us information within the next 12 months about the magnetic structure of cycle 21. In the event of two field reversals before the end of cycle 20, the Babcock dipole model would be invalidated.

Some studies by Steenbeck and Krause (1969) propose dynamo models which allow for the solid rotating core, the long period variations (80 - 100 years), the quadrupole structure observed at the peak of cycle 19, and may provide a basis for the 5-year fine structure in the butterfly diagram. It remains to be seen whether these particular models can account for a double negative magnetic cycle structure. Gilman (1968) is developing a model with heliostrophic flow in the solar convection zone, and with Rossby waves transferring momentum from the pole to the equator. Some of his models have demonstrated the property of not reversing magnetic polarity.

5.4 PLANETARY–SOLAR COUPLING MECHANISM

No specific coupling mechanism for the interaction of planetary resonances and the solar activity characteristics is presented here. The hypothesis that such a coupling mechanism is probably required is supported by the observed correspondence between inner planet resonance (11 years), outer planet resonances (180 years), and dominant periods in the solar cycle. Fine structure in the solar cycle time series has recently been correlated with cross-modulation products of the sidereal periods of the four largest planets (Bureau and Craine, 1970).

The mechanisms usually proposed are tidal forces or centrifugal forces due to the sun's motion about the center of gravity of the solar system. However, without a complete magneto-hydrodynamic treatment of the tidal problem, the theory is inadequate to explain the phenomenon. Lindzen (1970) has only recently applied the detailed hydromagnetic theory to "tides" in the earth's ionosphere. The results in the ionosphere yield slab motion and a complex latitudinal modal structure. Such a theory should be refined, applied to the sun's atmosphere and compared with sunspot latitudinal structure and motion.

The possibility of planetary-solar activity coupling has been studied by many authors. Evidence from recent studies indicates that such coupling is likely, based on statistical studies. All of this work, plus the improved statistics demonstrated in this study, indicate that a solar physical model requires a solar-planetary coupling mechanism.

5.5 A NEW TOPOLOGICAL MAGNETIC SOLAR MODEL

There is another solar-planetary coupling mechanism which may play a significant role in establishing the importance of solar-planetary interaction (Sleeper, 1971). The rigidly rotating core configuration studied by Howard, Wilcox, and Severny with a synodic rotation rate of 27.04 $\pm$ .02 days, compared with an equatorial "photosphere" rotation rate of ~ 26.8 days, is a very close integer multiple of 2 years: 27 x 27.04 = 730.08 days. This implies the possibility of spin-orbit coupling of the solar rigid rotating core and the earth's orbital period, analogous to possible spin-orbit coupling of Venus with the earth. The sun's spin may be trapped in an earth-orbital resonance.

The experimental work of Severny (1969), Wilcox et al. (1969), and Wilcox et al. (1970), plus the possible breakdown of the Babcock magnetic dipole model, leads to a hypothesis for a new double or multiple magnetic solar cycle model.

The basic model incorporates a rigidly rotating core, with a synodic spin period of 27.0 days, and a radius of about 0.9 R_θ. The convection zone is then divided into two major circulation zones, equatorial and polar (Figure

5-2). The point of division is 15 - 20 degrees latitude, or the region where the core and the convection zone have the same rotation rate. In the equatorial zone there is a convection cell which circulates downward at the equator, and thus moves in the opposite sense to the Hadley cell in the earth's atmosphere. The polar cells move downward at the poles. In the equatorial zone, within $\pm$ 20 degrees, the mean zonal flow is in the direction of rotation of the sun, and the relative period at the equator compared with the rigid core is 0.1-0.2 synodic days. In the polar zones the relative flow is opposite to the core rotation. The net result is transfer of momentum in the surface layer from the poles to the equator. The postulated photosphere motion is consistent with the observed sunspot longitudinal and meridional flow (Ward, 1965 and Coffey and Gilman, 1969).

Topologically, this model consists of two Babcock "dipole subcycles" in series during a single 11-year sunspot cycle. The initial subcycle is the conventional Babcock dipole model, with differential rotation producing a toroidal field of increased strength and buoancy, resulting in sunspot pair formation at high latitudes and then flare production. The flare production and associated "breaking" of toroidal field lines results in a reconnection of field lines in the lower latitudes, and the initiation of a second subcycle in the lower latitudes. Thus in the middle of a negative cycle, for instance, there is a combination of the residual toroidal field at high latitudes and the new dipolar field at low latitudes. The lower latitude zone then produces its own toroidal field due to differential rotation, and sunspots appear in the equatorial zone moving toward the equator. The magnetic topology of the new solar model is illustrated in Fig. 5-3. A third subcycle may be initiated in the equatorial zone. For negative cycles, these occur about once every Gleissberg cycle. For positive cycles, a residual third cycle occurs more frequently. As a result, Spoerer's law is an artifact, due to overlapping of sunspots from high and low latitude subcycles. This model has many of the characteristics of both Babcock's topological model (1961) and Allen's meridional circulation model (1960). A significant difference from Allen's model appears to be the nonoverlapping circulation zones. This model also appears to be qualitatively consistent with the experimental data presented by Rosenberg (1970).

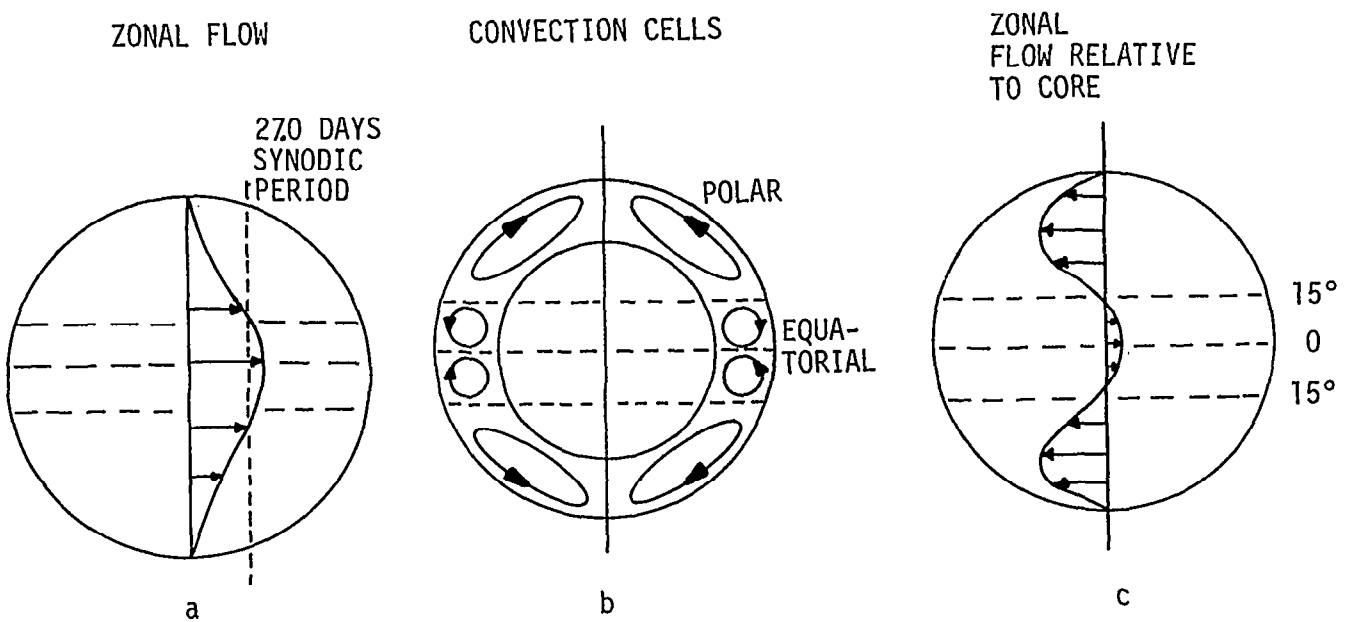

Figure 5-2. SOLAR FLOW STRUCTURE:MAGNETIC SUB-CYCLE MODEL

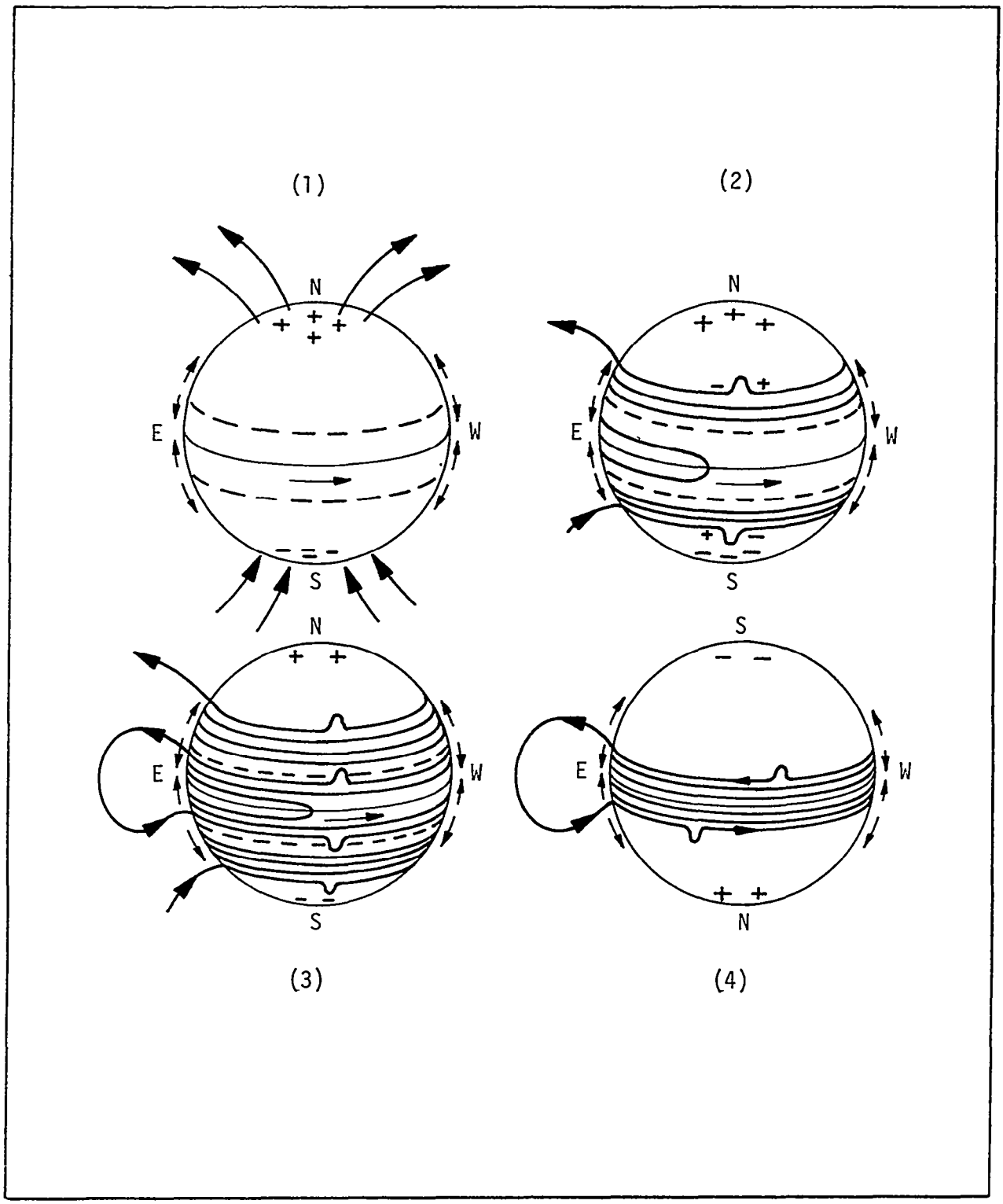

Figure 5-3. MAGNETIC TOPOLOGY FOR SUB-CYCLE MODEL

In addition to the convection zone controlled subcycles, there is a magnetic field "fine" structure associated with the nominally rigid core. Within the core, it is postulated that there are very slow convection circuits comparable with the nondipolar magnetic field convection loops in the earth's core. These loops account for the longitudinal sector structure in the core, either dipolar or quadrupolar, and may account for the preferred sunspot longitudes. This model accounts qualitatively for most of the observed phenomena, and is perhaps sufficiently complex to permit the anomalous behavior of two successive negative cycles.

Section VI

RECOMMENDATIONS

The results from this study suggest specific avenues for further empirical and analytical development for long-range solar activity prediction.

1. The model for sun-earth spin orbit coupling of the core should be studied. The observed oblateness of the sun may provide a mechanism for tidal coupling.

2. The solar dynamo theoretical model should be modified to provide a rigid core with a synodic rotation rate of 27.0 days and a latitudinally varying surface rotation rate.

3. The empirical analysis should be concentrated on studying the sunspot and magnetic subcycle structure. Planetary orbital resonance structure should be examined for correlation with Mode I and Mode II bi-stable oscillation states.

Section VII

REFERENCES

Alfven, H. and Arrhenius, G., "Structure and Evolutionary History of the Solar System, I.", Astrophysics and Space Science, 8, p. 338, (1970).

Allen, C. W., "A Sunspot Cycle Model" Observatory, 80, p. 94-98, (1960).

Antalova, A. and Gnevyshev, M. N., "Principal Characteristic of the 11-year Solar Activity Cycle", Soviet Astronomy, 9, p. 198-201, (1965).

Babcock, H. W., "The Topology of the Sun's Magnetic Field and the 22-year Cycle", Astrophys. J., 133, p. 572, (1961).

Bezrukova, A. Y., "On the Epoch of the Maxima of the Eleven Year Cycles 20, 21, and 22", Soln. Dannye, p. 69-74, (1962).

Bigg, E. K., "Influence of the Planet Mercury on Sunspots", Astron. J., 72, 463-466, (1967).

Blizard, J. B., "Long Range Solar Flare Prediction", NASA CR-61316, (1969).

Bonov, A. D., "Prognosis of the 11-year Cycles No. 20, 21, and 22 of the Solar Activity", Soln, Dannye, p. 68-73, (1968).

Boykin, E. P. and Richards, T. J., "Application of Lincoln-McNish Technique to the Prediction of the Remainder of the Twentieth Sunspot Cycle", LMSC/HREC-A782508, (1966).

Briér, G. W., Carpenter, T. H. and Cotton, B. F., "Time Series Analysis and Cycles in Geophysical Phenomena", 2nd Conf., Internat. Inst. for Interdiscip. Cycle Research, Roordwijk, Netherlands, June 1970.

Bureau, R. A. and Craine, L. B., "Sunspots and Planetary Orbits", Nature 228, p. 984, (1970).

Carpenter, R. L., "A Radar Determination of the Rotation of Venus", Astron. J., 75, pp. 61-66, (1970).

Coffey, H. E. and Gilman, P. A., "Sunspot Motion Statistics for 1965-67", Solar Physics, 9, 423-426, (1969).

Dodson, H. W. and Hedeman, B. R., "The History and Morphology of Solar Activity, 1964-1965", Annals of the IQSY, 4, The MIT Press, (1969).

Gilman, P. A., "Thermally Driven Rossby-Mode Dynamo for Solar Magnetic-Field Reversals", Science, p. 760-763, (1968).

Gleissberg, W., Terr. Magn. and Atm. Electr., 49, p. 243, (1944).

Goldreich, P., "Commensurable Mean Motions in the Solar System", Monthly Notices, Royal Astron. Soc., 130, p. 159, (1965).

Goldreich, P. and Peale, S., "Spin-Orbit Coupling in the Solar System", Astron. J., 71, p. 425, (1966).

Gray, Private Communication, (1970).

Hale, G. E., "On the Probable Existence of Magnetic Fields in Sunspots", Astrophys. J., 28, 315-343, (1908).

Howard, R., "Photospheric Magnetic Fields", Asilomar Solar Wind Conference, (1970).
Howard, R., (Private communication), (1972.)
Jose, P. D., "Sun's Motion and Sunspots", Astron. J., 70, 1965, pp. 193-200, (1965).

Kepler, J., "Harmonices Mundi Libri V", Lincii, Austriae, (1619).

King-Hele, D. G., "Prediction of Dates and Intensities of the Next Two Sunspot Maxima", Nature, 209, p. 285-6, (1966).

Kopecky, M., BAC, 2, p. 14, (1950).

Leighton, R. B., "A Magneto-Kinematic Model of the Solar Cycle", Astrophys. J. 156, p. 1-26, (1969).

Lincoln, J. V., "Smoothed Observed and Predicted Sunspot Numbers, Cycle 20", Solar-Geophysical Data, Sept. 1970, No. 313, Part I, p. 9, (1970).

Lindzen, R. S., "Internal Gravity Waves in Atmospheres With Realistic Dissipation and Temperature, Part I", Geophysical Fluid Dynamics, 1, p. 303-355, (1970).

Lindzen, R. S. and Holton, J. R., "A Theory of Quasi-biennial Oscillation", J. Atmos. Sci, 25, p. 1095-1107, (1968).

McNish, A. G. and Lincoln, J. V., "Prediction of Sunspot Numbers", Trans. Am. Geophys. Union. 30, No. 5, p. 673-685, (1949).

Molchanov, A. M., "The Resonant Structure of the Solar System", Icarus, 8, 203, (1968).

Molchanov, A. M., "Resonances in Complex Systems, A Reply to Critiques", Icarus, 11, 95-103, (1969a).

Molchanov, A. M., "The Reality of Resonances in the Solar System", Icarus, 11, 104-110, (1969b).

Portig, W. H. and Freeman, J. C., "Investigation of the Relation Between Solar Variations and Weather on Earth", Final Report, NASA Contract No. NASW-724, (1965).

Rosenberg, R. L., "Unified Theory of Interplanetary Magnetic Field", Solar Physics, 15, p. 72-78, (1970).

Severny, A., "Is the Sun a Magnetic Rotator", Nature, 224, pp. 53-54, (1969).

Sheeley, N. R. Jr., "Polar Faculae During the Sunspot Cycle", Astrophys. J. 140, p. 731-735, (1964).

Shuvalov, V. M., "Dependence of the Solar Cycle on the Position of the Planets", Astron. Vestnik, 4, pp. 198-203, (1970).

Sleeper, H. P., Jr., "Bi-Stable Oscillation Modes of the Sun and Long Range Prediction of Solar Activity", Northrop-Huntsville, TR-709, (1970).

Sleeper, H. P., Jr., "Long Range Prediction of Solar Activity", E.O.S., Trans. A. G. U., 52, No. 4, SS-20, (1971).

Sleeper, H. P., Jr., "Sun-Earth Spin Orbit Coupling", E.O.S., Trans. A. G. U., 52, No. 11, SS-27, (1971).

Slutz, R. J.; Gray, T. B.; West, M. L.; Stewart, F. G. and Loftin, M., "Solar Activity Prediction", Final Report, NASA-H-54409A, NOAA, Boulder, Col., (1970).

Steenbeck, M. and Krause, F., "Zur Dynamotheorie Stellarer und Planetarer Magnetfelder, I", Astron. Nach., 291, pp. 49-84 (1969).

Stenflo, J. O., "The Polar Magnetic Fields of July and August 1968", Solar Physics 13, p. 42-56, (1970).

Stewart, F. G. and Ostrow, S. M., "Improved Version of the McNish-Lincoln Method for Prediction of Solar Activity", I. T. U. Journal, 37, No. V, (1971).

Suda, T., "Some Statistical Aspects of Solar-Activity Indices", J. Met. Soc. Japan, 40, p. 287-299, (1962).

Vitinski, Y. I., "Solar Activity Forecasting", 1962, NASA-TTF, 289, (1962).

Vitinski, Y. I., "Solar Cycles", Solar System Research, 3, 99-110, (1969).

Waldmeier, "The Sunspot Activity in the Years 1610-1960, Zurich, Schulthess, (1961).

Ward, F., "Determination of the Solar Rotation Rate from the Motion of Identifiable Features", Astrophys. J., 145, pp. 416-425, (1966).

Weidner, D. K., "Natural Environment Criteria for 1975-1985 NASA Space Stations", NASA TMX-53865, 31 Oct. 1969.

Wilcox, J. M.; Severny, A. and Colburn, D. S., "Solar Source of Interplanetary Magnetic Fields", Nature, 224, pp. 353-4, (1969).

Wilcox, J. M.; Schatten, K. H.; Tanenbaum, H. S. and Howard, R., "Photospheric Magnetic Field Rotation; Rigid and Differential", Solar Physics 14, pp. 255-262, (1970).

Wood, K. D., "Long Range Solar Flare Prediction", see J. B. Blizard Denver Research Institute, NASA CR-61316, 1969, (1968).

Wood, R. M. and Wood, K. D., "Solar Motion and Sunspot Comparison", Nature 208, p. 129-31, (1965).

NASA-Langley, 1972 —— 30 M187